Long-term monitoring of environmental pollutants in the indoor climate of various housing types

Eindrapport

DEPARTEMENT OMGEVING

omgevingvlaanderen.be

Long-term monitoring of environmental pollutants in the indoor climate of various housing types

Deze studie …

[Korte samenvatting van opzet en/of resultaten van de studie]

Dit rapport bevat de mening van de auteur(s) en niet noodzakelijk die van de Vlaamse Overheid.

COLOFON

Verantwoordelijke uitgever

Peter Cabus

Departement Omgeving

Vlaams Planbureau voor Omgeving

Koning Albert II-laan 20 bus 8, 1000 Brussel

vpo.omgeving@vlaanderen.be

www.omgevingvlaanderen.be

Auteurs

Borislav Lazarov – VITO, Unit HEALTH

Bart Elen – VITO, Unit HEALTH

Maarten Spruyt – VITO, Unit HEALTH

Marianne Stranger – VITO, Unit HEALTH

Depotnummer

[Enkel bij gedrukte publicaties]

ISBN-nummer

[Enkel bij gedrukte publicaties]

Wijze van citeren

[Bij voorkeur volgens APA]

PARTNERS

MANAGEMENTSAMENVATTING

INHOUDSTAFEL

1 INTRODUCTION

The goal of this pilot study is to integrate low-cost electronic sensors into at least 3 sensor unit devices, to simultaneously assess various air pollutants in residences of the social housing sector and beyond. By means of an online 'intake' survey, occupant behaviour and housing characteristics are being inventoried. Sensors are being calibrated and verified, to explore the possibility to use the output data to evaluate Indoor Air Quality (IAQ) guidelines (such as the Flemish Indoor Environmental Decree) as well as other health-based reference values. Besides the direct communication of the sensor unit with the building occupants, measurement data will be coupled to an operational platform for online data transmission, where they will be collected in a database and related to information on housing and occupant behaviour. An algorithm for data-analysis and the design of an easy to use webpage for online follow-up of the measurements are also part of this project.

As described in the project proposal, LNE/OL201400032/15002/M&G the main objectives of this project include:

- The development of at least 3 sensor unit prototypes with electronic sensors for the continuous follow-up and evaluation of the indoor environmental quality (and possibly parameters of the outdoor environment)
- The development of a system for online registration and questionnaire-based surveys about housing characteristics and occupant behavior
- The developed monitoring units will show sensor readings on a display at a relevant frequency and will transfer collected data online (Wi-Fi network) to a database.
- The design of a central working unit (database) and data-analysis algorithm.
- The online visualization of monitoring results on a simple website as well as the offline analysis of monitoring data collected in a database.
- The organization of a test case in one house, demonstrations in several 'VMSW' houses, processing of the collected data.

The ambition is to equip each house with a sensor unit, of which in this pilot study 3 prototypes are being developed and optimized. Together with the installation of the sensor unit, an online survey on housing and occupant behaviour will be established. The illustration in Figure 1 demonstrates the set-up of the developments that will be created in this project.

Figure 1 Schematic set-up of the data collection in each house.

Content wise, the set-up of work packages in this project is based on the design illustrated in Figure 2.

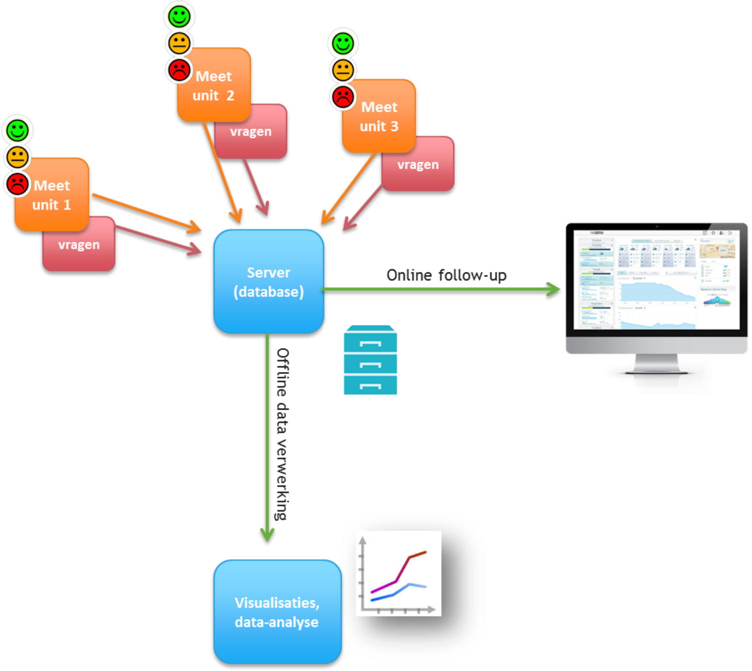

Figure 2 Schematic presentation of the communication between sensor units, server and output.

The sensor unit, consisting of an aggregation of electronic sensors, is referred to as the ‘indoor@box’. The indoor@box registers indoor environmental parameters on a house unit level. On the one hand, the unit has a direct communication with building occupants, by means of coloured LED indicators and a display presenting concise and simple messages. On the other hand, indoor environmental parameters, as well as responses to online surveys, will be communicated to a central server unit, in which they will be collected and saved in a database. Data in the database will be corrected based on calibration data and will then be visualized for online follow-up on a simple website. By means of a data processing algorithm, the monitoring data will be processed (on a basic way), with respect to building and occupant characteristics. These data will also be visualized on the project website.

2 INDOOR@BOX DEVICE

One of the objectives of this project is to design and develop a monitoring device, capable to integrate and manage selected “low-cost” electronic sensors for assessing the parameters defined in the project proposal (listed inTable 1)

Table 1 Parameters to be monitored by the sensor unit, according to the project proposal

TVOCs	Relative humidity
NO_2	Noise
CO_2	Light intensity
CO	Occupancy detection
PM	Electric energy consumption
Temperature	

During the development of this monitoring device, the following objectives and functionalities were considered:

- to be able to manage in terms of controlling and reading out the measurement responses of the selected “low-cost” electronic sensors for this project
- to allow a relatively easy reconfiguration of the set of sensors in terms of sensing parameters (by adding, removing or updating sensors)
- to be able to transfer the obtained sensor responses to the dedicated data collection infrastructure via secure internet connection
- to provide a high level of measured data integrity
- to provide a direct communication of the outcomes to occupants, by means of coloured LED indicators and a display showing concise and simple messages.
- to reach as high as possible accuracy and resolution for sensor responses

Keeping these objectives in mind, the following technical solutions were adopted; listed in the same order as the list of objectives:

- Considering the variety of the available sensors and their controlling and data communication protocols, a dedicated micro controller (e.g. ATMega2560) was used to provide the control and data acquisition of the sensors.
- The indoor@box devices were designed as a modular device which consists of three major units (modules): (1) sensor controller unit – containing the required sensor and the supporting electronics for sensor control and data acquisition; (2) processing unit – providing data management in terms of data storage and its secure transportation to a dedicated data collection infrastructure, and (3) user interface unit – providing direct communication of the obtained measurements to the occupants. All three units communicate using a standard UART serial communication protocol. The modular design allows individual reconfiguration of a single module without interrupting the device integrity.
- The device was designed to provide internet connectivity via wired and/or wireless connection. The transport of measured data to a dedicated data collection infrastructure is realized by means of Secure File Transfer Protocol (SFTP). More information about data transfer and data collecting infrastructure is provided at Chapter **3** of this report.
- The integrity of measured data is guaranteed by additional storage of all output data from the sensors, locally to the device, using a non-volatile SD memory card.

- To visualize the readings from the sensors, the indoor@box device is equipped with LCD display where the outcomes of selected sensors are displayed. Additionally, a simple algorithm which displays easy (short and easily understandable) pre-defined-messages, considering the condition of the indoor environment, based on the IAQix index calculated from the outcomes from the sensors and the requirements for healthy IAQ stated in the Vlaamse Binnenmilieubesluit (2018), is developed and implemented.
- All the electronic components in this project were selected considering the optimal balance between price and quality in order to improve the stability and reduce the electrical noise. To provide high electronic resolution for the sensors with analog output, a 16-bit analog to digital (A/D) converter with programmable gain amplifier is used. The gain amplifier is used to boost up smaller signals to a full range and increasing the resolution of the measurement.

The architecture of the indoor@box device is given in Figure 3.

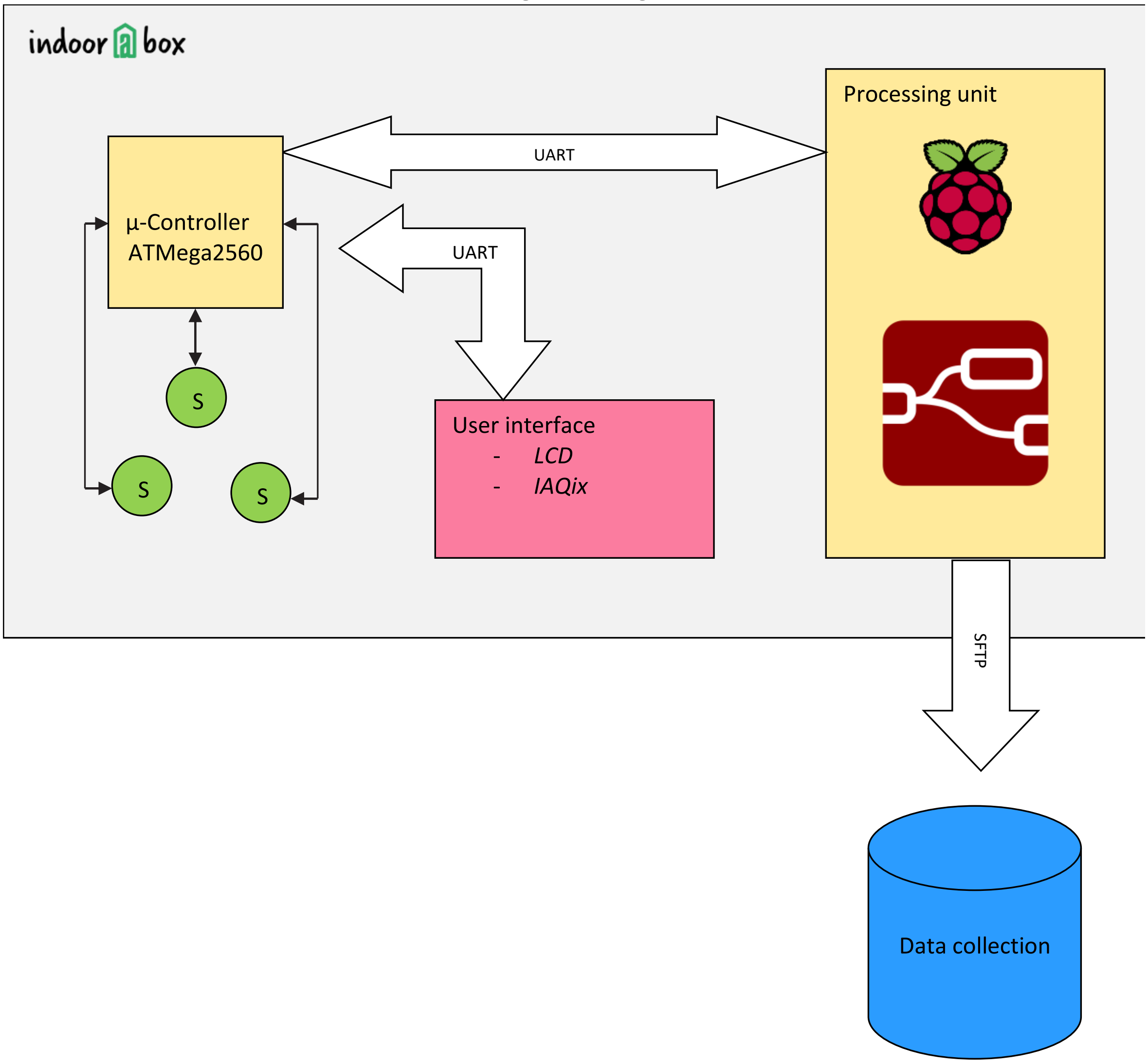

Figure 3 A block schematic overview of the indoor@box device architecture

2.1 TECHNICAL DESCRIPTION OF THE INDOOR@BOX' SENSOR CONTROLLER

The sensor controller unit of the indoor@box device was designed with the following specifications:

- 3 analogous output sensors for measuring TVOCs, CO and NO_2.
- 4 digital output sensors for measuring CO_2, temperature and humidity, PM and occupancy
- Wireless (RF433MHz) communication capability to receive data from an auxiliary measurement module (e.g. energy consumption).
- Serial communication capability for communication with an external, wired auxiliary measurement module (e.g. noise and light intensity)
- an ATMega2560 processor, running at 16 MHz
- a linear power regulator for 5V
- USB-to-serial communication

The block schematic overview of the sensor controller is illustrated in Figure 4. The solid arrows in the overview mark data flow direction. The architecture of the sensor controller unit can be divided into five sections: sensors with analogous output, sensors with digital output, wireless (RF433MHz) communication module, wired communication module and a micro-controller. All five sections are integrated in a single printed circuit board, integrated in the indoor@box device. The full electrical scheme of the sensor controller unit is presented in Annex A

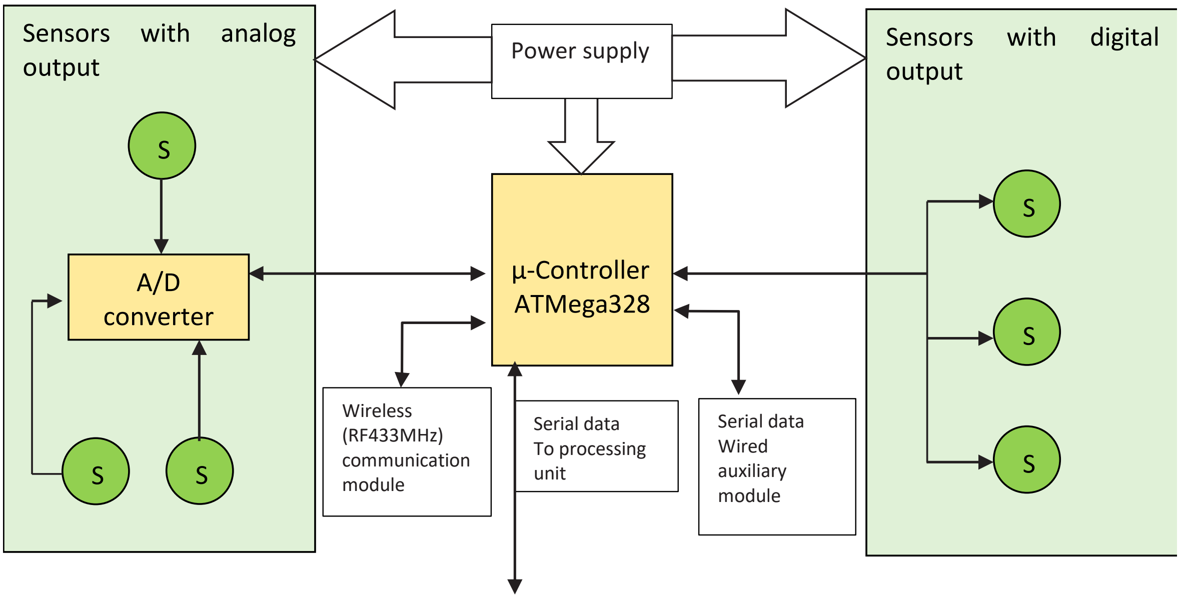

Figure 4 A block schematic overview of the Indoor@box's sensor controller architecture

2.1.1 Sensors with analog output

This section includes the sensors which produce continuous analog output (voltage or current) proportional to the measurement outcome. The output signal of each individual sensor is connected to an A/D converter in order to translate the analog signal from the sensor to a digital one which can then be used for further processing and storage. 16-bit A/D converters (TI ADS1115 (Texas Instruments, 2017)) have been used for this particular application. TI ADS1115 is 4-channel 16-bit analogous to digital converter, with an internal reference, oscillator and programmable comparator. The programmable gain amplifier of the A/D converter provides up to 16 times gain for low voltage analogous signals, allowing to keep a good resolution of the measurements. The communication with the A/D converter is made through a standard 2-wire I2C bus. The individually selectable address of the A/D converter allows up to 4 of these devices to be individually controlled on the same I2C bus, giving a total number of 16-single ended or 8 differential analog channels to be measured. The power characteristic of ADS 1115 shows that the converter is 5V tolerant, which makes it suitable for direct integration to the 5V power architecture of the sensor controller.
The sensors with analogous output, selected for this project are: the TVOCs sensor (PID-AH2, Alphasense); the carbon monoxide sensor (CO-B4, Alphasense) and the nitrogen dioxide sensor (NO2-B4, Alphasense). All sensors are rated from their manufactures to be 5V compatible, therefore they can be directly integrated to the 5V power architecture of the indoor@box' sensor controller.

2.1.2 Sensors with digital output

The other types of sensors used in this project are sensors with a digital output i.e. the measurements are directly communicated from the sensor as a digital signal. The advantage of digital output sensors is that all the electronics for controlling the sensor and measuring the signals are embedded in a single package, which lowers possible interferences from the electronics. Moreover, for most of the digital output sensors, the built-in support electronics is optimized by the manufacturer to provide optimal working conditions of the sensor and to reduce the interferences of external factors.

The used digital output sensors in this project are: CO_2 sensor (EE983, E+E Elektronk), temperature and relative humidity sensor (SHT75, Sensirion), light intensity sensor (TSL2561, AMS), occupancy detection sensor (MDU1100T, Microwave Solutions), as well as electricity consumption measuring modules (emonTx V3, OpenEnergyMonitor). The communication protocol and power characteristics of each sensor are individually defined by their manufacturer and in most of the cases well documented in the technical information accompanying the sensor. Therefore, the communication and power characteristics of each of the selected digital output sensors are individually described in following paragraphs.

2.1.2.1 Carbon dioxide

EE983 miniature CO_2 sensor module from E+E Elektronik (Figure 5) is fully equipped with the necessary controlling electronics to maintain independently (without additional controlling equipment) optimal operational conditions. The measured data from the EE983 CO_2 sensor are available on custom and well the documented E2 digital interface based on I2C bus introduced by Philips Semiconductors (now NXP Semiconductors) in 1982 (http://www.nxp.com/docs/en/user-guide/UM10204.pdf). According to the information provided from the manufacturer, the sensor operates at power supply voltage between 4.75V and 7.5V, which makes it suitable for direct integration to the 5V power line of the sensor controller unit.

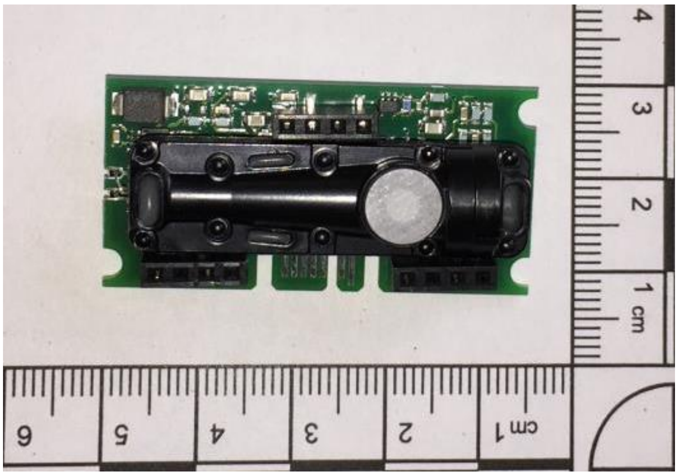

Figure 5 EE983 digital CO_2 sensor module (E+E Elektronik)

2.1.2.2 Temperature and relative humidity

SHT75 temperature and humidity sensor (Figure 6) from Sensirion integrates in a single chip temperature and humidity sensor, analogue-to-digital converter, a calibration memory and a digital interface which guarantees excellent reliability and long term stability. The data communication with the sensor is available via a well-documented 2-wires serial interface (Sensirion, 2011). The sensor operates at power supply between 2.4 and 5.5V, which makes this sensor suitable for direct integration to the 5V power architecture of the sensor controller unit.

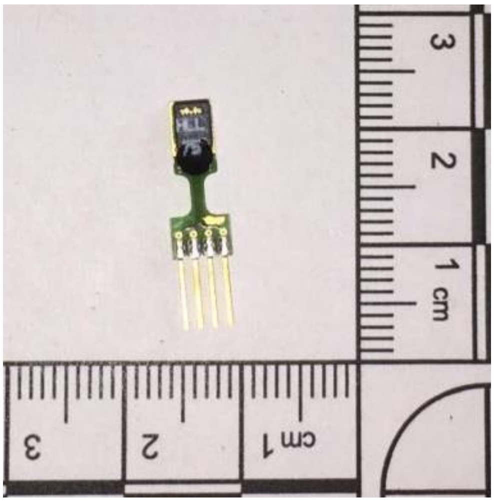

Figure 6 SHT75 temperature and humidity sensor (Sensirion)

2.1.2.3 Light intensity

TSL2561 light sensor (Figure 7) from AMS selected for this project is a dual photodiode sensor capable for simultaneous measurements of IR, full spectrum or human visible light. The built-in precise A/D converter and programmable signal amplifier (gain) makes the sensor capable to detect light ranges from up to 0.1 to 40 000 lux. The sensor operates at a supply voltage between 2.7 and 3.6V, therefore a linear power regulator and logic level converter have been included in order to be able to implement the sensor in the 5V logic level architecture of the sensor controller unit. The communication with the sensor is performed using standard I2C communication protocol (http://www.nxp.com/docs/en/user-guide/UM10204.pdf).

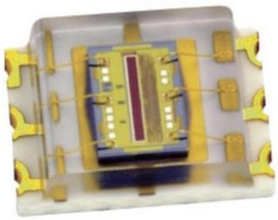

Figure 7 TSL2561 light intensity sensor (AMS)

2.1.2.4 Occupancy detection

A microwave motion/occupancy sensor MDU1100T from Microwave Solutions is used to detect the occupancy within 10 meters around the indoor@box. The sensor uses a Doppler Effect microwave detection method for sensing movements of objects within detection zone. The sensor works at 10.525 GHz microwave frequency and according to the information provided by the manufacturer it complies with the requirements in EN 300 440 European standard for short range radio equipment devices used in the 1GHz to 40GHz frequency range (ETSI EN 300 440, 2017). According to the information provided from the manufacturer, the microwave radar sensor operates at supply voltage of 5V which makes it suitable for direct integration to the 5V power architecture of the sensor controller unit.

2.1.2.5 Electricity consumption

To measure the parameter electricity consumption of either the entire dwelling or a specific appliance, a commercially available measurement system (emonTX V3, OpenEnergyMonitor) was used. EmonTX V3 is a fully calibrated stand-alone module for monitoring the electricity consumption of up to four single-phase circuits using non-invasive, clip-on CT sensor technology. The module uses a low power 433MHz radio to transmit the measurement data to receiving station via a standard universal asynchronous receiver/transmitter (UART) serial communication protocol. According to the information provided from the manufacturer, the radio receiver interface is described to be not 5V tolerant (it uses 3.3V power architecture), therefore a linear power regulator and logic level converter have been included in order to be able to implement the receiver into the 5V logic level architecture of the sensor controller unit.

2.1.3 Micro-controller

The central element of the sensor controller unit is the micro-controller ATMega2560 (Microchip, 2016). It provides all the necessary setups for an optimal operation for each individual sensor. It also retrieves, filters and averages the responses of the sensors and transfers them to the processing unit via serial communication line. The commercially available product Crumb2560 V1.1

AVR ATmega Module (https://www.chip45.com/index.php) implements an ATMega2560 micro-controller, a USB-to serial adapter and a power regulator in a single 61x30.5 mm printed circuit board. The micro-controller can receive a firmware by the on-board serial connector through an USB to Serial adapter compatible with the Arduino framework and integrated development environment (IDE).
For this project Crumb2560 module operates at 16MHz with 5V logic level and is implemented as a central micro-controller element for the sensor controller unit. The integration of three main components (ATMega2560 microprocessor, a USB to serial adapter and a voltage regulator) in a single relatively small board makes Crumb2560 module very suitable for prototyping purposes, where the design might be often changed. Furthermore, the built-in USB to serial adapter of Crumb2560 module allows communication with the sensor controller unit and real time acquisition of the data from the sensors (e.g. during laboratory calibration) without the need of the processing unit using a TTL serial interface. However, as the data communication lines (serial Tx0 and Rx0) are shared between USB to serial adapter of the Crumb2560 and the communication interface with the processing unit, the sensor controlling unit must be disconnected from the processing unit during uploading new firmware in the micro-controller through the build in USB to serial adapter.

2.2 TECHNICAL DESCRIPTION OF THE INDOOR@BOX PROCESSING UNIT

The processing unit of the indoor@box is realised using the commercially available single board computer platform - Raspberry Pi 3 (https://www.raspberrypi.org/). Raspberry Pi 3 integrates a quad-core 1.4GHz CPU, 1GB RAM, Wi-Fi and Bluetooth low energy connections, 4 USB ports and Micro SD port for memory card for loading the operating system and storing data. The system uses specifically developed for this platform Debian-based Linux operating system. The operating system is available under GNU General Public License (www.gnu.org).
The indoor@box processing unit uses a flow-based programming tool (Node-Red https://nodered.org/) to read the data available on the serial communication port from the sensor controller unit and structuring them in a CSV file. The transfer of the obtained measurement results to the dedicated online data storage location is performed via secure file transfer protocol (SFTP). To provide additional level of securing the measurement data, the processing unit saves a copy of the raw measurements into its memory card.
The internet connectivity of the indoor@box is realized either via the build in Wi-Fi communication module or the Ethernet port of the processing unit. Both methods required physical internet access point at the measurement location (LAN, Wi-Fi or 3G via WLAN mobile router).

2.3 USER INTERFACE

The indoor@box device provides three major ways for direct communication of the outcomes to the occupants i.e. LCD User Interface, IAQix Colour Interface, and indoor@box Dashboard Interface.

2.3.1 LCD user interface

The LCD user interface of indoor@box is realized with 4.3'' capacitive touch TFT LCD display module from 4D Systems. The build in processor and non-volatile memory storage allow the module to manage and store independently pre-configured user interface designs for displaying information. The display information is received to the module via standard UART serial communication protocol. In addition, the capacitive touch sensor of the display allows interaction with the indoor@box device. The LCD user interface is realized with five main screens *Home Screen*, *User Feedback Screen*, *Measurements Screen*, *Carbon Monoxide Alarm Screen*, *Info Screen*. A brief overview of the sections and the data presentation on the screens is shown below.

2.3.1.1 Home Screen

Figure 8 indoor@box LCD user interface – Home Screen

An example of the indoor@box LCD user interface's Home screen is shown in Figure 8. The main purpose of this screen is to display a simple and easy to understand overview of the data obtained from the sensors at the last measurement. The *Home Screen* includes the following sections:

a. Text representation of the calculated IAQix index
b. Pictogram representation of the calculated IAQix index
c. "Fresh Air" indicator calculated based on measured CO_2 concentration
d. Value of the temperature obtained at the last measurement
e. Relative Humidity value obtained at the last measurement
f. Internet status indicator
g. User Feedback Screen activation button

2.3.1.1.1 Textual representation of the calculated IAQix index (see 2.3.1)

This section provides a textual representation of the calculated IAQix index. The text variations corresponding to each IAQix index levels are shown in Table 2.

Table 2 Text representation of the different IAQix index levels

IAQix level A	UITSTEKENDE LUCHTKWALITEIT
IAQix level B	GOEDE LUCHTKWALITEIT
IAQix level C	MATIGE LUCHTKWALITEIT
IAQix level D	SLECHTE LUCHTKWALITEIT

2.3.1.1.2 Pictogram representation of the calculated IAQix index

This section represents the IAQix index levels in the form of pictograms. The pictograms used to represent the different IAQix index levels are shown in Table 3.

Table 3 Pictogram representation of the different IAQix index levels

 IAQix level A	 IAQix level B	 IAQix level C	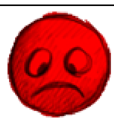 IAQix level D

2.3.1.1.3 "Fresh Air" indicator

The "Fresh Air" indicator was developed and used to visualize the CO_2 concentration levels measured by the indoor@box devices. The indicator uses 10 level scale, realized with bar graphs (Table 4), to indicate the amount of "fresh air" in the indoor environment. In the context of this indicator, a "fresh air" is an outdoor air with average CO_2 concentration levels of 350 – 500 ppm. The "Fresh Air" level indicator is calculated based on the measured CO_2 concentration, according to equation *1*.

$$FAI = \frac{(c_{CO2} - CO2_{min}) * (FAI_{max} - FAI_{min})}{(CO2_{max} - CO2_{min}) + FAI_{min}} \qquad 1$$

where

FAI is the "Fresh Air" indicator level
c_{co2} is the CO_2 concentration measured by the indoor@box device
$CO2_{min}$ is the min CO_2 concentration level (100% "fresh air")
$CO2_{max}$ is the max CO_2 concentration level (0% "fresh air")
FAI_{min} is the min value of the FAI index (i.e. 1)
FAI_{max} is the max value of the FAI index (i.e. 10)

Table 4 “Fresh Air” level indicator

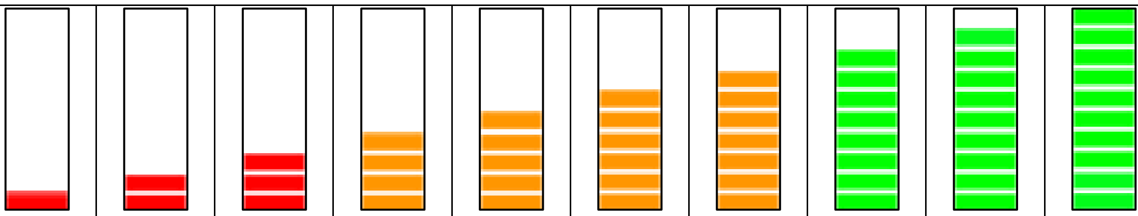

1	2	3	4	5	6	7	8	9	10

For the current project, the $CO2_{min}$ and $CO2_{max}$ were set to 500 ppm and 2000 ppm, respectively.

2.3.1.1.4 Internet status indicator

The internet status indicator (Table 5) provides information for the availability of an active internet connection of the indoor@box device. The indicator checks only for an active connection established between the indoor@box device and a dedicated online server in internet and does not provide information regarding the connection to the local network.

Table 5 Internet status indicator

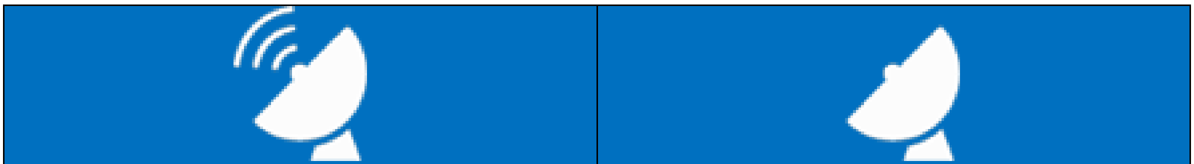

The device has active internet connection	The device does not have active internet connection

2.3.1.2 User Feedback Screen

Figure 9 indoor@box LCD user interface – User Feedback Screen

A simple 3 levels pictogram together with a simple question (Figure 9) is used to interact with the occupants in order to receive their feedback regarding their perception of IAQ. The information of their feedback is communicated back to the processing unit and stored to the CSV file together with the other measurement data.

The *User Feedback Screen* includes the following sections:

a. Pictogram representing the 3 level occupants’ feedback regarding their perception of IAQ
b. Selection indicator
c. Conformation button

2.3.1.3 Measurements Screen

Figure 10 indoor@box LCD user interface – Measurements Screen

The *Measurements Screen* (Figure 10) provides numeric representation of the concentrations of selected parameters measured during the last measurement cycle. The values in this screen are updated every time when a measurement cycle is completed. No historical data from previous measurements is shown in this screen.

2.3.1.4 CO Alarm Screen

Figure 11 indoor@box LCD user interface – Carbon Monoxide Alarm Screen

In case of high levels of CO concentrations detected, the device enters into CO alarm mode. During this mode, the *Carbon Monoxide Alarm Screen* (Figure 11) is activated and remains active as long as the CO alarm mode is active. The CO alarm mode of the indoor@box device is activated when the measured CO concentration is above 10 mg/m³ for at least 60 min (i.e. 20 consecutive measurements at 3 min measurement interval).

2.3.1.5 Info Screen

Figure 12 indoor@box LCD user interface – Info Screen

The *Info Screen* (Figure 12) provides contact information of the owner of the indoor@box device. The screen includes also the device Shut Down button (a) and the Wi-Fi reset button (b).

a. indoor@box device shut down button
b. Wi-Fi reset button
c. Confirmation button (activates the Home Screen)

2.3.2 IAQix colour interface

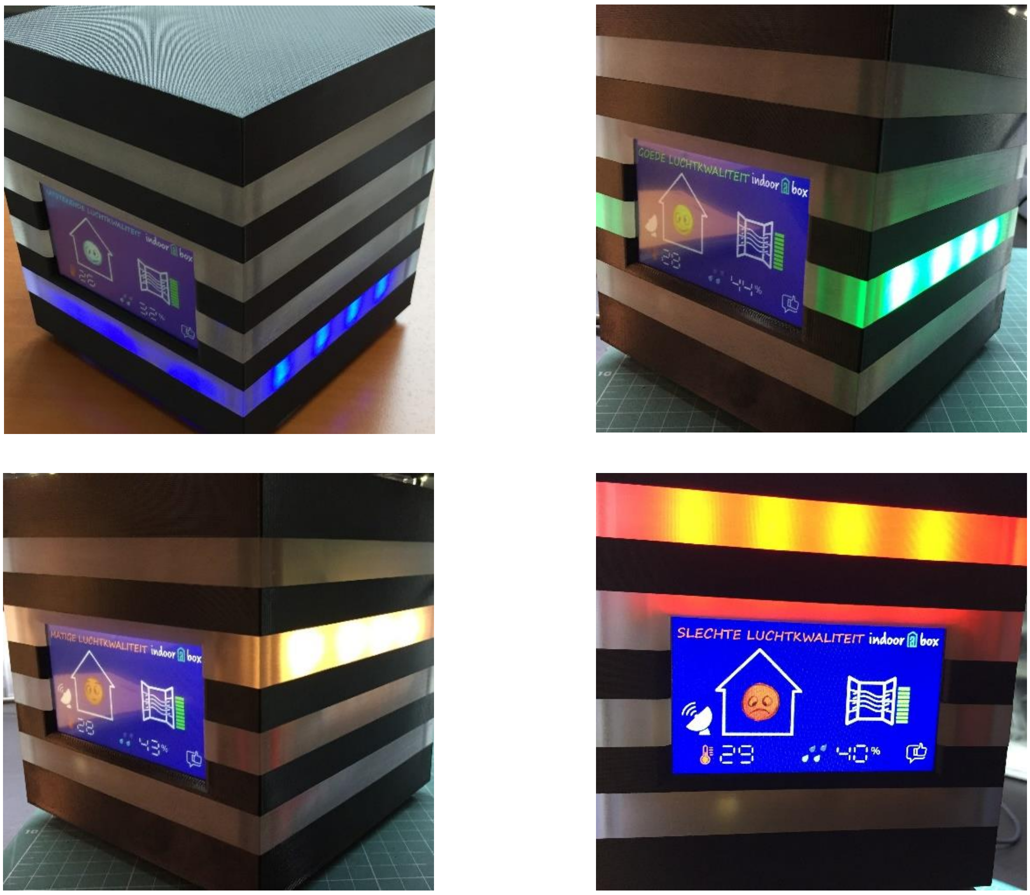

Figure 13 indoor@box's IAQix color interface

For ambient air-quality, a comprehensive air-quality index (CAQI) is already used in several EU member states to present the polluted level of the air; people can thereby easily identify the status of air-quality. However, unlike the CAQI for ambient air-quality that is regulated nationally or regionally, it is difficult to define CAQI for indoor air-quality, since the criteria of air-quality vary according to the indoor environment (e.g., home, parking station, factory, etc.).

For the purpose of the indoor@box project a simple IAQ index (IAQix) has been developed based on the existing approaches for computing air quality indexes, taking also into consideration the guide and intervention values of indoor air pollutants listed in the Vlaamse Binnenmilieubesluit (2018). A detailed description of the IAQix calculating algorithm is given in Annex C. The resulted 4 levels of IAQix index are represented as a colour light rings embedded in the indoor@box enclosure (Figure 13). The illuminated light colour of each of the ring corresponds with the colour assigned for the IAQix index i.e. Blue (IAQix level A - Good), Green (IAQix level B - Moderate), Orange (IAQix level C - Unhealthy), and Red (IAQix level D - Very Unhealthy). A separate colour illumination ring is dedicated for each of the four IAQix levels to physically separate the indication levels to be easy recognizable also from colour-blind users.

2.3.3 indoor@box dashboard interface

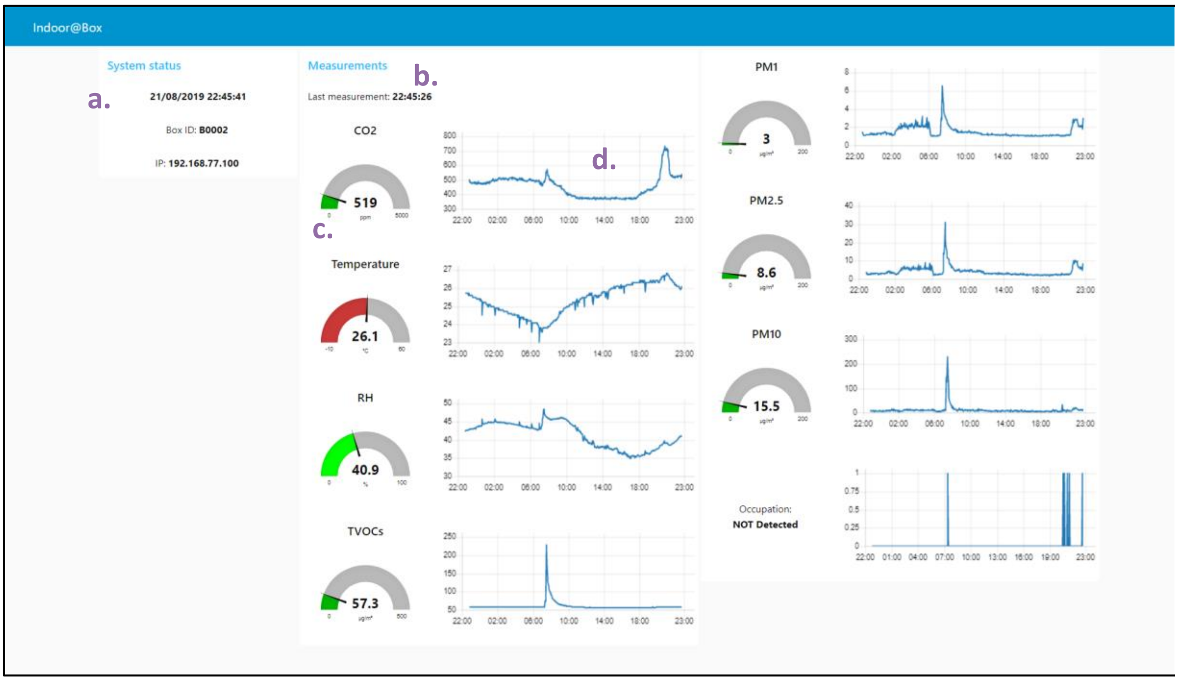

Figure 14 indoor@box dashboard interface

Every indoor@box device provides also a web-based dashboard, accessible only locally to each device. The indoor@box web-based dashboard (Figure 14) provides information specific only to the current indoor@box device, such as:

a. System information:
   - current date and time of the system
   - indoor@box's identification number
   - current IP address of the indoor@box device
b. Time stamp of the last performed measurement cycle
c. Numeric values of the outcomes obtained from the sensors at the last performed measurement cycle
d. Historical data of the measurement performed in the last 24h

The indoor@box dashboard interface is accessible only through the local (ethernet) network, where the device is connected to.
To access the indoor@box dashboard interface, a web browser of a computer connected to the same local (ethernet) network as the indoor@box device needs to be navigated to the following address:

http://*indoor@box_IP_address*:1880/ui

where, the *indoor@box_IP_address* is the IP address of the indoor@box device assigned from the DHPC server in the network.

2.4 PRINCIPLE OF OPERATION OF INDOOR@BOX

2.4.1 Communication within the indoor@box

The communication between the sensor controlling unit and processing unit of indoor@box follows the master/slave communication model, where the processing controller unit is the master while the sensor controller unit and the user interface are the slaves. Figure 15 shows the flow chart of the communication logic within the indoor@box monitoring device.

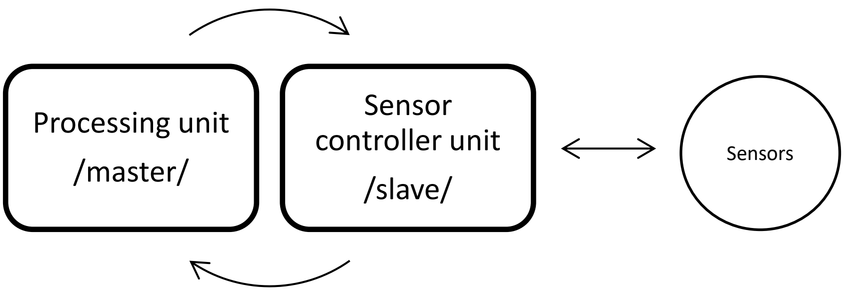

Figure 15 Flow chart of the communication logic

The communication within the indoor@box is always initiated and controlled by the processing unit (master). The main timing parameter for indoor@box is the measurement period, defined as a time interval in which one measurement value for each parameter is stored in the CSV file. This parameter is user defined, and for this project it is set to 3 min referring to a single cycle of measurement.

The flow of the performed steps for single cycle of measurement is described as follows:

1. At the start of a user pre-defined measurement period (measurement cycle), the processing unit (master) sends a command to the sensor controlling unit (slave) to read all the sensors.
2. After receiving the “start” command, the sensor controlling unit follows the sensor measurement routine (described in section 2.4.2) to obtain the readings from each sensor as follows:
    a. The micro-controller activates all the sensors for measurement
    b. The micro-controller acquires the raw output signal from each individual sensor
    c. The micro-controller performs a set of basic statistical operations (e.g. averaging multiple measurements) and stores a single averaged output value from each sensor to a buffer ready to be read from the processing unit.
    d. The newly obtained values are also sent to the user interface unit to be displayed on the LCD display.
3. When available at the buffer of the sensor controlling unit, the data are read by the processing unit. The processing unit marks the received values with a progressive timestamp and stores them into a CSV file following pre-defined structure and file name.
4. Every CSV data file is created on a daily base (separate data file every 24h) and stored in a non-volatile SD memory card. A copy of the complete daily CSV file is then sent to a dedicated data storage infrastructure using SFTP protocol.

The communication between both units is made through a UART serial line running at 9600bps, 8bit, no parity at 5V logic level (TTL) for the sensor controller and 3.3V for the processing unit. The sensor controller unit (slave) could accept set of commands from the processing unit (master) following a custom developed protocol described in Annex B.

2.4.2 Operation of the sensor controller unit

The flow chart presented in Figure 16 shows the operational logic for an individual sensor within the sensor controller unit. This flow is applied to all sensors of the controller unit. The solid arrows in this flow chart mark data flow direction.

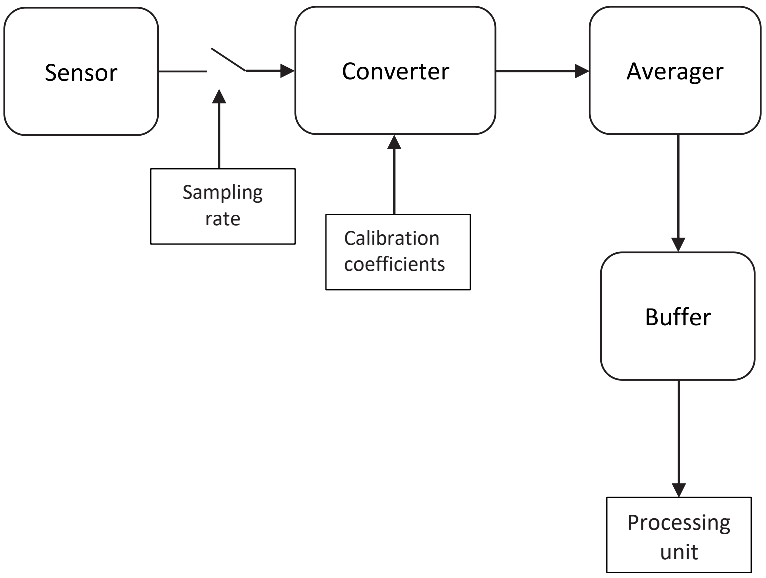

Figure 16 Flow chart of the firmware logic

Where:

- Sampling rate of the sensor represents the number of measurements performed by the sensor during one measurement cycle. This parameter defines the number of measurements from the sensor which will be averaged to a single output value from this sensor per measurement period.
- The convertor performs basic mathematical calculation to convert the raw signal (e.g. voltage) from the sensor into the required parameter. In this step the obtained during lab calibration conversion coefficients for the specific sensor are used.
- During the average step, the converted multiple measurements are averaged to a single output value for this parameter.
- The averaged values of the measurements are stored in a buffer and ready to be read from the processing unit.

The instructions that provide control, monitoring and data manipulation of the sensors are part of the developed for this project firmware, which is uploaded to the micro-controller via the build in USB to serial converter. All instructions (e.g. control, communication) and parameters (e.g. calibration coefficients, conversion factors) are pre-defined for each sensor and saved in the non-volatile memory embedded on the ATMega328. Therefore, in case of powering up the sensor controller unit or after reset, the micro-controller reads all the parameters from the non-volatile memory and automatically sets up the hardware.

3 DATA-COLLECTION AND DATA-VISUALIZATION

The goal of work package 3 is to design a data infrastructure with support for data collection, data transmission, data storage in a database, automated data processing, and data visualization through a web interface. This chapter gives an overview of the indoor@box data infrastructure and its individual components.

3.1 REQUIREMENTS

The key requirements for the data infrastructure are:

- **High reliability**: The risk of losing data at any part of the data infrastructure needs to be minimized.
- **High adaptability**: In a research context, changes to the data infrastructure will frequently be required. For instance, when a new type of measurement device or sensor is added, when new insights are gained in how to better process a sensor signal, or when the need for a new kind of online data analysis arises.
- **High reusability**: A new measurement campaign, even if done with similar measurement devices, does often come with its own requirements and goals. The data infrastructure must be designed to support reuse of software components from project to project and from measurement campaign to measurement campaign.
- **High scalability**: Measurement campaigns with a large number (hundreds) of measurement devices must be supported at every part of the data infrastructure.

3.2 SOFTWARE ARCHITECTURE

The following figure gives an overview of the architecture of the data infrastructure. It shows its components and the relationships between them.

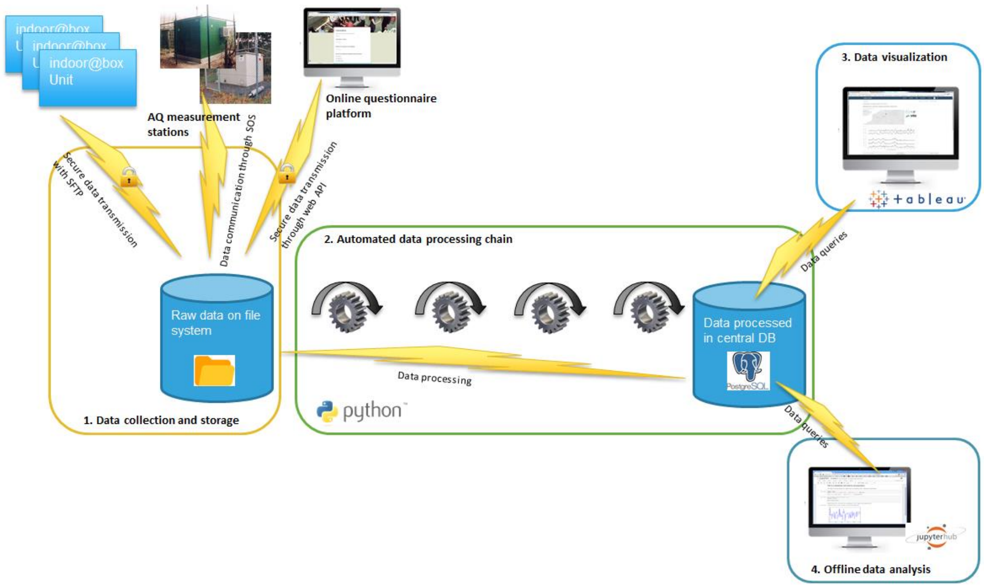

Figure 17 Overview figure of the data infrastructure

The key components of the data infrastructure are:
1. Data collection and storage: Automated data collection is required for a number of data sources. There are the Indoor@box measurement boxes collecting a wide range of indoor measurements, the measurement stations of the official Belgian air quality measurement networks, and the online questionnaire platform. The raw data collected from the data sources is stored in CSV files on the file system in a structured manner, as discussed in section 3.4.

a. **Indoor@box:** Secure data communication with the indoor@box measurement devices is realized with SFTP. Periodically (daily) each Indoor@box finishes a measurement file in CSV format and transmits it over the internet to a designated location (discussed in section 3.4) on the SFTP server. The design of the Indoor@box is realized in WP2.
b. **AQ measurement stations**: Up-to-date measurement data from the three official air quality measurement networks in Belgium (Vlaamse Milieumaatschappij, Agence wallone de l'air & du climat, and Bruxelles Environnement) is periodically downloaded from the IRCEL servers. The data communication is realized through a Sensor Observation Service (SOS), a web service to query sensor data, and part of the Sensor Web Enablement (SWE) standards.
c. **Online questionnaire platform**: The data collected by the online questionnaire is periodically downloaded through a web API. Secure communication with the web API is realized by the usage of HTTPS. The realization of the online questionnaire platform is discussed in more detail in section 3.3.

2. Automated data processing chain: The automated data processing chain stores and processes the data in the database with the help of reusable tools. The automated data processing chain is discussed in section 3.5, while the database design is discussed in section 3.6.

3. Online data visualization: The processed data is made available online through an online data visualization, implemented with Tableau. The online data visualization is discussed in section 3.7.

4. Offline data analysis: The processed data, stored in a PostgreSQL DB, needs to be analysed. A JupyterHub server has been set-up to enable, semi-automated, data analysis.. The actual data analysis will be done in WP4.

3.3 ONLINE QUESTIONNAIRE PLATFORM

For the creation of the online questionnaire platform, a selection had to be made between the numerous commercial and free software solutions available to create such a platform. To guide the selection process, an overview has been made of the wanted properties for the online questionnaire platform:

- With good web API to allow automatic data extraction from online questionnaire platform
- Easy to use (filling in questionnaires)
- Easy to alter questionnaires or create new questionnaires (should not require expert knowledge)
- Easy to set-up
- Support for a variety of question types
- Support for automated check if input value is valid
- Easy control of user rights
- Support for tablets
- Appealing look-and-feel
- Cheap (preferably free)

We chose Google Forms over other popular alternatives such as Surveymonkey and Surveygizmo due to its very good web APi and overall ease of usage. This free product is able to meet all current requirements for the online questionnaire platform. The questionnaire data is downloaded periodically in an automated way from Google Forms. We chose to download and store the raw questionnaire data in CSV file format for consistency reasons.

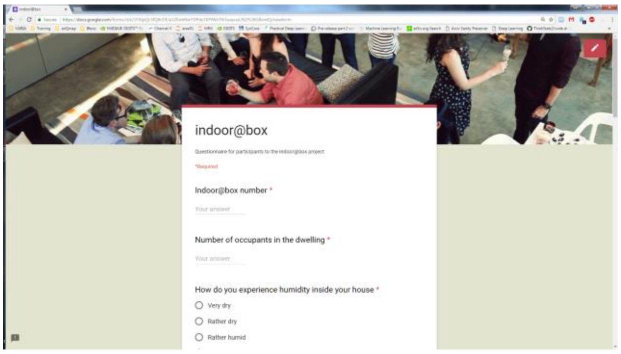

Figure 18 Screenshot from online indoor@box questionnaire, implemented on Google Forms

3.4 STORAGE OF RAW DATA

We chose to store the raw data from the indoor@box 's, the online questionnaires and the official Belgian air quality networks in CSV files on hard drives in a structured manner. This approach has a number of advantages: 1. It makes it very easy to manually add data files when automated data transmission has failed, e.g. due to a failing internet connection on the measurement location. 2. Realizing a periodic back-up of the raw becomes very easy; it can for instance be realized by storing the raw data files on a daily backed-up network drive.

The raw data has been structured as follows on the file system:

- "Data": The folder containing all raw collected data
    - "projectName1": The folder containing all raw data from a single project
    - "ProjectName2"
        - "MeasurementCampaign1": The folder containing all raw data from a single measurement campaign
        - "MeasurementCampaign2"
            - "DataSource1": The folder containing all raw data from a single data source. The currently supported data sources are: "ircel", "indoor@box", and "online questionnaire".
            - "DataSource2"
                - "MeasurementDevice1": The folder contains all raw data from a single measurement device
                - "MeasurementDevice2"
                    - "DataFile1": CSV file containing the actual raw data
                    - "DataFile2"

All projects, measurement campaigns, data sources, and measurement devices get a short, descriptive, unique ID. Those ID's are used in the folder names and in the database in a consistent manner. The measurements of AQ monitor "40AL01" from "Ircel" during the pilot measurement campaign ("cp0)" of project "lne" can for instance be found in following folder:

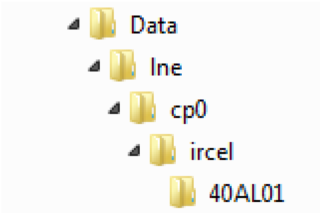

Figure 19 Example location on file system where the raw measurement files of a single measurement device are stored

All measurements from measurement devices belonging to the same 'data source' class are processed by the same data processing chain. For this reason, measurement devices belonging to the same data source are expected to collect quite homogeneous data. They are allowed to vary from each other in number of sensors, but they should measure the same component similar on all devices. E.g. if one measurement device has a high-quality temperature sensor which measurements do not require any post processing, then this should be the case for the temperature measurements of all measurement devices within the same data source class.

The name of the CSV files with raw data contains the measurement device ID and the measurement date and is structured as follows: "MeasurementDeviceID_YYYY-MM-DD.csv". For each measurement device a separate data file is expected for every day of measurements.

3.5 AUTOMATED DATA PROCESSING CHAIN

The automated data processing chain processes the raw data into data fitted online data visualization and for further analysis. Processing of the data is, as much as possible, done directly on the database. This approach allows high performance and should scale well to very large datasets. The automated data processing chain is implemented in Python 3.5. The written Python code has been made compliant with the PEP 8 style guide for Python code.

A helper class called "DbData" is created to make it easy to work with data stored in the database. It contains useful functionalities and information such as, the database connection object, helper functions to load and store pandas data frames from and to the database, and configuration information to create the database connection.

The data processing steps are implemented as independent "tools". Those tools are combined in a "data processing chain". Implementing the data processing as a chain of reusable tools makes it easier to create a new, custom, data processing chains for future measurement campaigns. We can expect new measurement campaigns to require some modifications to the data processing. For instance, because changes have been made to the used set of sensors, or due to differences in the envisioned end-goal. All tools are implemented as separate Python modules which can be loaded independently. Each tool expects as input a DbData object offering access to the data it has to work on.

The data processing tools are grouped in Python packages to keep a better overview. The current packages are:

1. **Extract**: Tools to extract the data from external data sources (e.g. online questionnaire platform).
2. **Load**: Tools to load data from one data source into the database.
3. **Process**: Tools to do data processing on data from an individual data source (e.g. data filtering, smoothing, calibration, aggregation, …)
4. **Synchronize**: Tools to combine data from different data sources in a synchronized manner.
5. **Enrich**: Tools to create new information by combining data.
6. **Export**: Tools to export data (e.g. to a CSV file, to a report, to a web server, …)

3.6 DATABASE DESIGN

The database is structured as follows:

- A separate database schema is created for each project to contain all project data. This way, a clear separation of data is realized between projects. This allows to implement access control for the different stake holders at DB schema level. Also, project data can be easily archived at the end of the project. If multiple measurement campaigns are done within the same project, their data is stored in the same database schema.
- All database tables in the project schema can be created automatically based on the raw data stored on the file system. The raw data from measurement devices of the same data source are stored in the same database table. One database table with raw data is created for each data source (indoor@box 's, IRCEL, online questionnaire platform, …).
- For some data sources, additional meta information is available. For instance, for the IRCEL AQ measurement stations, we know their latitude and longitude coordinates, their station area type (urban, suburban, rural), which city is in the neighbourhood, etc. This meta information can be considered static. For this reason, it is stored in a separate “meta” schema.
- We chose to store the intermediate results of the data processing chain in the database. They can offer valuable information to better understand how certain end-results have been obtained. The name of each database table contains a reference to the project, measurement campaign and the different data processing steps applied on the data in the table. The database tables are named as follows: “projectID_measurementCampaignID_processingStep1ID_processingStep2ID_...”. For instance, the table “lne_cp0_ircel_meta” contains data of the “lne” project of the pilot measurement campaign “cp0” from the “ircel” data source with “meta” information added to the measurements.

3.7 ONLINE DATA VISUALIZATION

The measurements from the indoor@box’s will be available through a web interface created in Tableau. Currently, no measurements have been collected yet with the indoor@box’s. The first online dashboards created with Tableau visualize outdoor air quality measurements from IRCEL. Since the IRCEL data is public data, the created dashboards can currently still be hosted, for free, on Tableau Public. As soon as more private data must be made available online, yearly licenses will need to be purchased from Tableau.

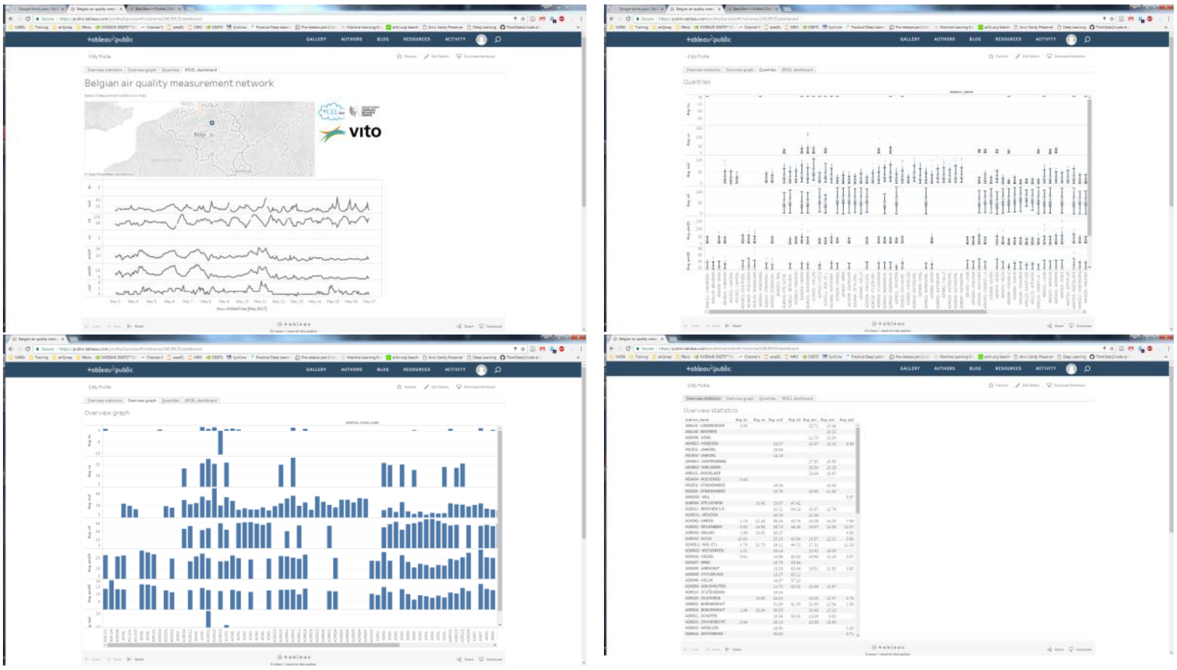

Figure 20 Interactive online dashboards visualising air quality measurements from IRCEL

4 PERFORMANCE TESTING OF INDOOR@BOX

The last part of the study was dedicated to the assessing the performance of the developed indoor@box monitoring devices under controlled (laboratory) as well as in real indoor environmental conditions. To achieve this goal, several laboratory and field tests have been organized and executed during the project.

The field test experiments were organized in two main approaches:

- ***Initial field test*** was organized and executed in a selected indoor environment, where the available indoor@box devices were running simultaneously to estimate a potential deviation of the overall measurements between the devices.
- ***Reference field test*** where indoor@box monitoring devices were installed at selected indoor environments and operated together with reference discontinue measurement instruments to estimate the compatibility between the measurement of indoor@box devices and the reference methods.

4.1 LABORATORY TEST

As a first step of the performance testing of the developed indoor@box devices, the performance of the individual sensors was assessed under controlled (laboratory) conditions.

Figure 21 Laboratory test configurations

4.1.1 Exposure test chamber

The evaluation of the indoor@box devices under controlled (laboratory) conditions were performed inside closed stainless-steel exposure test chamber (Figure 21). The total internal volume of the chamber of 117 dm³, provided enough space for testing up to three indoor@box devices simultaneously. The homogeneity of the chamber's inner atmosphere was supplied by the build-in mixing fan. The temperature and relative humidity inside the exposure test chamber were constantly monitored and recorded using calibrated T/RH monitor (Testo 175H1, with accuracy of 0.4°C and 2% RH). The T/RH measurements were recorded as a minute averages.
The chamber was supplied with a constant flow of carrier gas at rate of 30 L/min. The gas molecule residence time *t* inside the chamber for used carrier gas flow rate (30 L/min) and total volume of 117 L was estimated at 3.67 min, calculated by Eq. *2*

$$t = \frac{V}{Q} = \frac{117\,L}{30\,\frac{L}{min}} = 3.67\,min \qquad 2$$

Where,

t is the residence time of the gas molecules inside the exposure test chamber, min
V is the volume of the exposure chamber, L
Q is the total carrier gas flow through the exposure test chamber, L/min

To reach a steady-state condition inside the chamber, 2 – 3 residence times are needed, resulting to a total of about 8 – 11 minutes.

4.1.2 Gas mixtures generation

Dried, clean air or pure nitrogen were used as carrier gases during the laboratory tests. The carrier gas was humidified to the desired humidity level prior entering the exposure test chamber using a Bronhorst controlled evaporator mixer (Bronhorst CEM EVAPORATOR W-202A). This instrument provided constant and controlled humidity between 5% and 90% RH.
The gaseous target parameters were produced using two methods depending of the compound. CO, CO_2, and NO_2 were produced by diluting gas of known (certified) concentration from a gas cylinder with pollutant free air or pure nitrogen. Precise mass flow controllers were used to control the target and diluting gas flows. A three-way valve was used to add the desired gas mixture to the humidified carrier gas flow before entering the exposure chamber.
The standard VOC test mixture was produced by control evaporation of a solvent mixture of target compounds and mixing it with the humidified carrier gas of the chamber. Pressurized air was used to control the flow of the solvent VOC mixture through a capillary column to the evaporator. The VOC concentration generated during the experiments were calculated via the weight of the solvent mixture introduced to the exposure chamber.
The VOC gas mixture was added to the humidified carrier flow via three-way valve prior entering the exposure test chamber.

4.1.3 PM generation

The PM inside the exposure test chamber was generated by PALAS Particle dispenser system (PALAS) using Dolomite dust. The particle loaded airflow from the dispenser was then inject into the mixing duct, where the particles were mixed with filtered (particle free) air (Figure 22). A portion of the mixed air was then sampled through the Venturi feed and injected to the inner atmosphere of the exposure chamber. The rest of the mixed particle loaded air in the mixing duct

was vented. The concentration of the particles injected to the exposure test chamber could be controlled either through the feed of the particle dispenser system or by the dilution input through the Venturi feed.
The actual concentration and particle size distribution inside the exposure test chamber was monitored using a calibrated optical particle counter (GRIMM 11, particle size range: 0.253 – 35.15 µm, 0 µg/m³ - 100 mg/m³, reproducibility: ±3% for total measuring range).

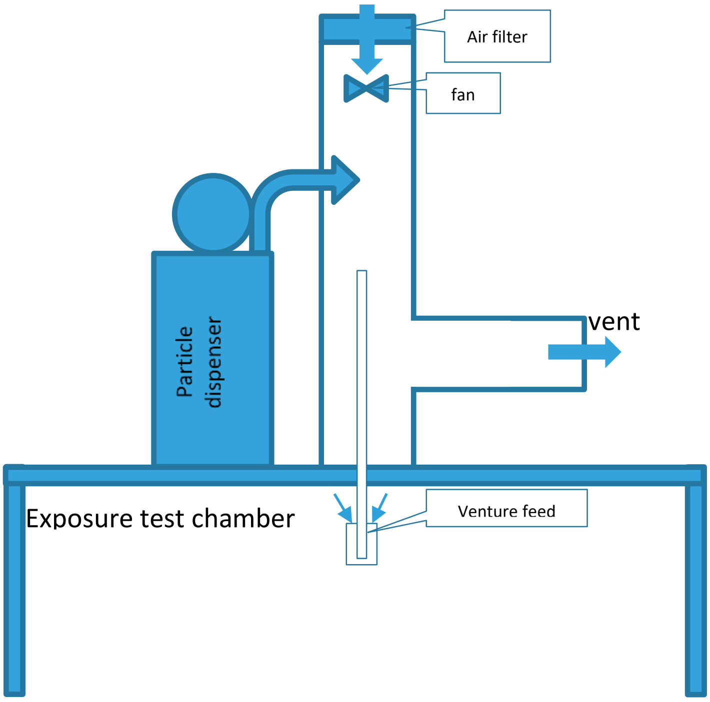

Figure 22 Schematic of particle generation and distribution system

4.1.4 Measurement instruments

All gas flows during the experiments were controlled using high accuracy mass flow controllers (EL-FLOW SELECT, Bronhorst). All gas flows were measured using calibrated flow meters (Gilian Gilibrator-2 NIOSH Primary Standard Air Flow Calibrator, Sensidyne and DryCal 1020 Primary Flow Calibration Standard, Mesa Labs).
The reference continuous and semi -continuous gas and PM monitors used to conduct gas and PM measurements during the laboratory tests were:

- Calibrated optical particle counter (GRIMM 11, particle size range: 0.253 – 35.15 µm, 0 µg/m³ - 100 mg/m³, reproducibility: ±3% for total measuring range) was used to assess the concentrations of PM1, PM2.5 and PM10 fractions in the inner atmosphere of the exposure chamber during the performed PM tests.
- Calibrated real-time trace (ppb) level NOx analyser (Thermo, resolution 0.4 ppb) was used measure the NO_2 concentrations of the inner atmosphere of the exposure test chamber during the performed experiments.
- Calibrated NDIR based CO_2 monitor (CATEC, 0 – 5000 ppm) was used for assessing the CO_2 concentrations inside the exposure test chamber during the performed experiments.
- Calibrated T/RH monitor/logger (Testo 175H1, accuracy of 0.4°C and 2% RH) was used during the performed experiments to log the temperature and relative humidity inside the exposure test chamber

4.1.5 Linear correlation

The linearity of the individual sensors included in the indoor@box device to the corresponding target parameters were evaluated. For this, the indoor@box devices were exposed to the target parameters at pre-defined levels at controlled environment (exposure test chamber). The response of each individual sensor was evaluated for at least 5 individual levels (L0 – L4) for each parameter following the sequence shown in Table 6 (except for PM).

Table 6 Linearity correlation testing sequence

Step	Test level of the targeted parameter	Temperature	Duration
1	L0	25 ± 1 °C	≥ 60 min
2	L1	25 ± 1 °C	≥ 60 min
3	L0	25 ± 1 °C	≥ 60 min
3	L2	25 ± 1 °C	≥ 60 min
4	L0	25 ± 1 °C	≥ 60 min
5	L3	25 ± 1 °C	≥ 60 min
6	L0	25 ± 1 °C	≥ 60 min
7	L4	25 ± 1 °C	≥ 60 min
8	L0	25 ± 1 °C	≥ 60 min

To assess the linearity of the relationship between the output from an individual sensor and the corresponding target parameter, a regression analysis was applied. For this, the best fitting regression curve was calculated along with the corresponding correlation coefficient (R^2), slope and intercept values.

4.1.5.1 PM sensor

The linearity of the PM sensors of the indoor@box devices were tested following the sequence and conditions shown in Table 7. The listed concentrations of the different concentration levels are targeted values, the concentrations of the PM fractions inside the exposure chamber during the experiments were measured by the reference instrument (GRIMM). The PM concentrations for each concentration level were presented as an average of the measured concentrations for a steady state period of 20 min. The concentrations obtained from the tested PM sensors were calculated as an average for the same steady state period.

Table 7 Linearity correlation testing conditions for PM

Step	Concentration level	PM1, µg/m³	PM2.5, µg/m³	PM10, µg/m³	Temperature	RH	Duration
1	L0	0	0	0	25 ± 1 °C	2 – 3 %	≥ 30 min
2	L1	3	10	20	25 ± 1 °C	2 – 3 %	≥ 30 min
3	L2	4	20	40	25 ± 1 °C	2 – 3 %	≥ 30 min
4	L3	6	40	60	25 ± 1 °C	2 – 3 %	≥ 30 min
5	L4	8	50	80	25 ± 1 °C	2 – 3 %	≥ 30 min
6	L5	10	60	100	25 ± 1 °C	2 – 3 %	≥ 30 min
7	L6	12	70	120	25 ± 1 °C	2 – 3 %	≥ 30 min

Figure 23 shows a graphical presentation of the performed linear regression analysis for different PM fractions of the PM sensors of the tested indoor@box devices.

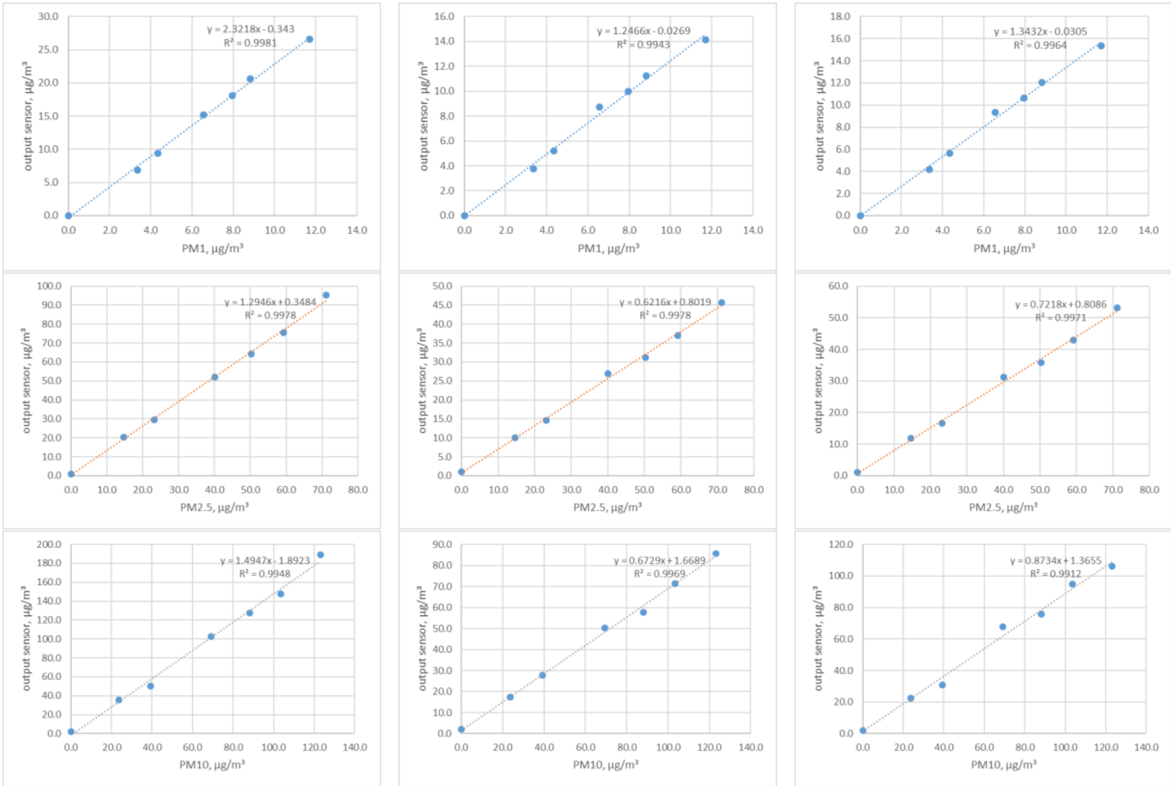

A B C

Figure 23 Graphical presentation of the linear regression analysis of the PM sensors of the tested indoor@box devices: B0001 (A); B0002(B) and B0003(C)

The outcomes from the test showed that the tested PM sensors have very good linear correlation ($R^2 > 0.990$) with the measurements performed by the reference instrument in controlled (laboratory) conditions (Table 8).

Table 8 R^2 linear correlation coefficients of the PM sensors of the tested indoor@box devices

indoor@box ID	PM1	PM2.5	PM10
B0001	0.9981	0.9978	0.9948
B0002	0.9943	0.9978	0.9969
B0003	0.9964	0.9971	0.9912

4.1.5.2 Carbon dioxide (NDIR) sensor

The linearity of the NDIR sensor installed in the indoor@box devices and used for measuring CO_2 concentrations were tested according the conditions presented in Table 9. For this experiment the 3-min (one measuring cycle of the indoor@box devices) average data from each period of a steady-state pollutant concentration in the chamber (usually the last 30 minutes from set of conditions) was considered for this analysis.

Table 9 Linearity correlation testing conditions for CO_2 (NDIR) sensor

Step	Concentration level	Carrier gas	Target CO_2 concentration, ppm	Temperature	RH	Duration
1	L0	N_2	0	25 ± 1 °C	50 ± 5 %	≥ 60 min
2	L1	N_2	400	25 ± 1 °C	50 ± 5 %	≥ 60 min
3	L0	N_2	0	25 ± 1 °C	50 ± 5 %	≥ 60 min
4	L2	N_2	1000	25 ± 1 °C	50 ± 5 %	≥ 60 min
5	L0	N_2	0	25 ± 1 °C	50 ± 5 %	≥ 60 min
6	L3	N_2	2000	25 ± 1 °C	50 ± 5 %	≥ 60 min

7	L0	N_2	0	25 ± 1 °C	50 ± 5 %	≥ 60 min
8	L4	N_2	4000	25 ± 1 °C	50 ± 5 %	≥ 60 min

Figure 24 shows a graphical presentation of the performed linear regression analysis of the CO_2 (NDIR) sensors of the tested indoor@box devices.

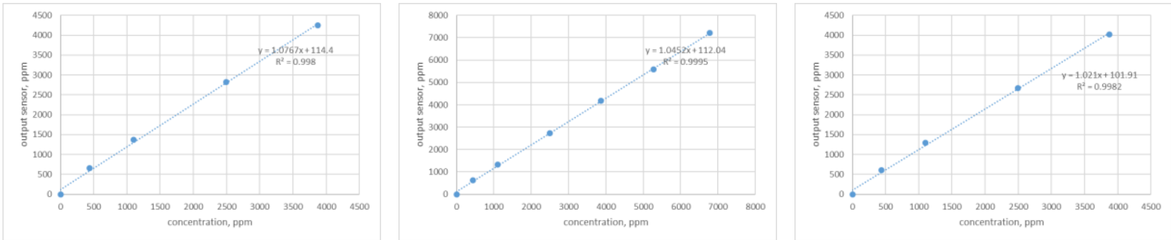

A B C

Figure 24 Graphical presentation of the linear regression analysis of the CO_2 sensors of the tested indoor@box devices: B0001 (A); B0002(B) and B0003(C)

Table 10 shows the obtained during this test, R^2 linear correlation coefficients for the tested sensors. The results showed correlation coefficients greater than 0.990 for all tested devices.

Table 10 R^2 linear correlation coefficients of the CO_2 sensors of the tested indoor@box devices

indoor@box ID	CO_2
B0001	0.9980
B0002	0.9995
B0003	0.9982

4.1.5.3 Carbon monoxide sensor

As most of the electrochemical gas sensor, the used in the indoor@box CO sensor have two raw outputs, including active (WE) voltage from the working electrode and reference (AUX) voltage from the auxiliary electrode. The WE voltage responds to target gas concentration directly and is also affected by environmental parameters, while the AUX voltage serves to anchor the working electrode voltage with response only to the change of environmental parameters. The difference of the WE and AUX voltage is proportional to the target gas concentrations. Therefore, for this analysis the difference between the WE and AUX voltage will be used as an output signal from this sensor. The conditions under which the CO sensor was tested are shown in Table 11. In this experiment, the resulted, reference CO concentration levels in the exposure test chamber were calculated considering the CO concentration in the gas bottle and the applied dilution factors. All flows were measured using calibrated, reference flow meters. In this experiment the 3-min (one measuring cycle of the indoor@box devices) average data from each period of a steady-state pollutant concentration in the chamber (usually the last 30 minutes from set of conditions) was considered for this analysis.

Table 11 Linearity correlation testing conditions for CO sensor

Step	Concentration level	Carrier gas	Target CO concentration, mg/m³	Temperature	RH	Duration
1	L0	N_2	0	25 ± 1 °C	50 ± 5 %	≥ 60 min
2	L1	N_2	0.8	25 ± 1 °C	50 ± 5 %	≥ 60 min
3	L0	N_2	0	25 ± 1 °C	50 ± 5 %	≥ 60 min
4	L2	N_2	1.5	25 ± 1 °C	50 ± 5 %	≥ 60 min
5	L0	N_2	0	25 ± 1 °C	50 ± 5 %	≥ 60 min
6	L3	N_2	3.0	25 ± 1 °C	50 ± 5 %	≥ 60 min

7	L0	N_2	0	25 ± 1 °C	50 ± 5 %	≥ 60 min
8	L4	N_2	6.0	25 ± 1 °C	50 ± 5 %	≥ 60 min

Graphical representations of the linear regressions obtained during the current CO sensor testing are shown in Figure 25

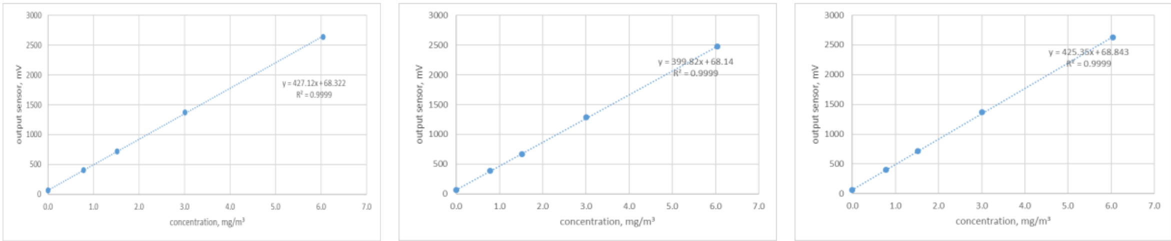

A B C

Figure 25 Graphical presentation of the linear regression analysis of the CO sensors of the tested indoor@box devices: B0001 (A); B0002(B) and B0003(C)

The obtained R^2 linear correlation coefficients of the tested devices are shown in Table 12

Table 12 R^2 linear correlation coefficients of the CO sensors of the tested indoor@box devices

indoor@box ID	CO
B0001	0.9999
B0002	0.9999
B0003	0.9999

4.1.5.4 Nitrogen dioxide sensor

The electrochemical NO_2 sensors included in the indoor@box devices, similarly to the CO sensors, provide two (WE and AUX) voltage outputs. The difference between both signals is also the parameter which is proportional to the concentration of the target pollutant (NO_2). Therefore, for this analysis the difference between the WE and AUX voltage will also be used as an output signal from this sensor type. The conditions of the performed tests are shown in Table 13Table 11. Identically to the other tests, the 3-min (one measuring cycle of the indoor@box devices) average data from each period of a steady-state pollutant concentration in the chamber (usually the last 30 minutes from set of conditions) was considered for this analysis.

Table 13 Linearity correlation testing conditions for NO_2 sensor

Step	Concentration level	Carrier gas	Target NO_2 concentration, mg/m³	Temperature	RH	Duration
1	L0	N_2	0	25 ± 1 °C	50 ± 5 %	≥ 60 min
2	L1	N_2	0.8	25 ± 1 °C	50 ± 5 %	≥ 60 min
3	L0	N_2	0	25 ± 1 °C	50 ± 5 %	≥ 60 min
4	L2	N_2	1.5	25 ± 1 °C	50 ± 5 %	≥ 60 min
5	L0	N_2	0	25 ± 1 °C	50 ± 5 %	≥ 60 min
6	L3	N_2	3.0	25 ± 1 °C	50 ± 5 %	≥ 60 min
7	L0	N_2	0	25 ± 1 °C	50 ± 5 %	≥ 60 min
8	L4	N_2	6.0	25 ± 1 °C	50 ± 5 %	≥ 60 min

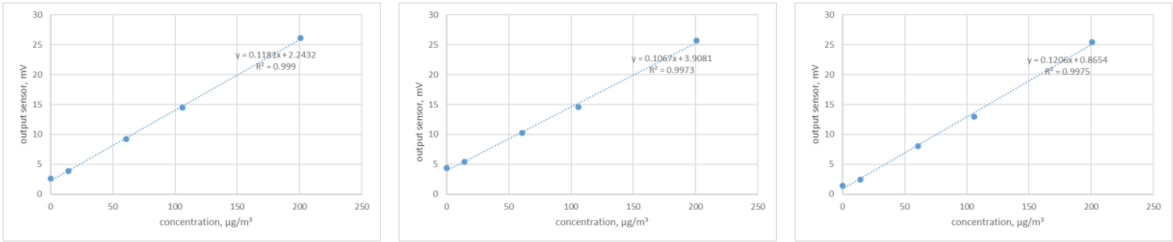

A B C

Figure 26 Graphical presentation of the linear regression analysis of the NO_2 sensors of the tested indoor@box devices: B0001 (A); B0002(B) and B0003(C)

Figure 26 shows graphical representations of the linear regressions obtained during the current NO_2 sensor testing. The obtained R^2 linear regression coefficients are shown in Table 14.

Table 14 R^2 linear correlation coefficients of the NO_2 sensors of the tested indoor@box devices

indoor@box ID	NO_2
B0001	0.9999
B0002	0.9999
B0003	0.9999

4.1.5.5 Temperature and humidity sensor

The linearity of the T/RH sensor installed in the indoor@box devices were tested in according the conditions presented in Table 15. For this experiment the 3-min (one measuring cycle of the indoor@box devices) average data from each period of a steady-state temperature and RH in the chamber (usually the last 30 minutes from set of conditions) was considered for this analysis.

Table 15 Linearity correlation testing conditions for T/RH sensor

Step	Test level	Carrier gas	Temperature	RH	Duration
1	L0	Zero Air	22	70	≥ 60 min
2	L1	Zero Air	24	70	≥ 60 min
3	L2	Zero Air	26	70	≥ 60 min
4	L3	Zero Air	28	70	≥ 60 min
5	L4	Zero Air	30	70	≥ 60 min
6	L5	Zero Air	50	30	≥ 60 min
7	L6	Zero Air	30	80	≥ 60 min
8	L7	Zero Air	30	70	≥ 60 min
9	L8	Zero Air	30	60	≥ 60 min
10	L9	Zero Air	30	50	≥ 60 min
11	L10	Zero Air	30	40	≥ 60 min
12	L11	Zero Air	50	30	≥ 60 min
13	L12	Zero Air	50	20	≥ 60 min
14	L13	Zero Air	50	10	≥ 60 min

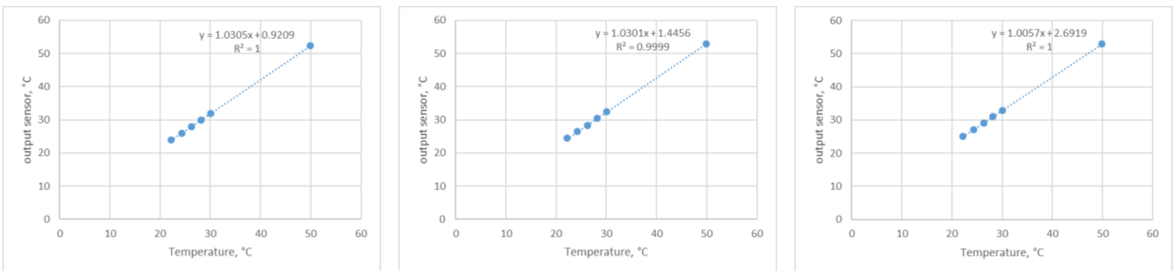

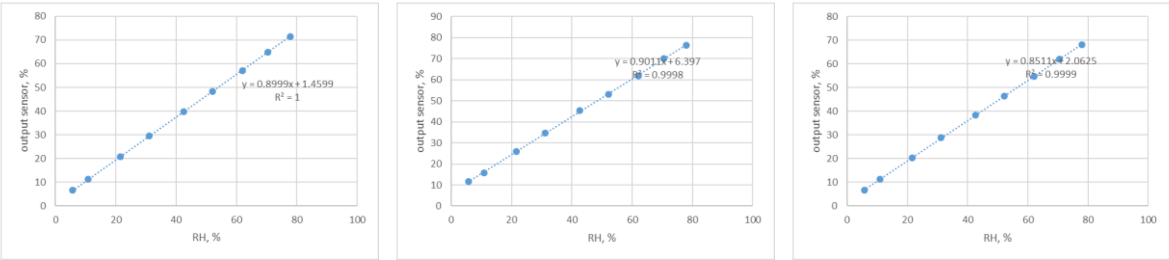

A B C

Figure 27 Graphical presentation of the linear regression analysis of the T/RH sensors of the tested indoor@box devices: B0001 (A); B0002(B) and B0003(C)

Figure 27 shows graphical representations of the linear regressions obtained during the current T/RH sensor testing. The obtained R^2 linear regression coefficients are shown in Table 16.

Table 16 R^2 linear correlation coefficients of the T/RH sensors of the tested indoor@box devices

indoor@box ID	T	RH
B0001	1.0000	1.0000
B0002	0.9999	0.9998
B0003	1.0000	0.9999

4.1.5.6 TVOC (PID)sensor

The linearity of the TVOC (PID) sensor of the indoor@box devices were tested following the sequence shown in Table 17.

Table 17 Linearity correlation testing conditions for TVOC (PID) sensor

Step	Test level	Carrier gas	TVOC, µg/m³	Temperature	RH	Duration
1	L0	Zero Air	0.0	25 ± 1 °C	50 ± 5 %	≥ 60 min
2	L1	Zero Air	100	25 ± 1 °C	50 ± 5 %	≥ 60 min
3	L2	Zero Air	200	25 ± 1 °C	50 ± 5 %	≥ 60 min
4	L3	Zero Air	800	25 ± 1 °C	50 ± 5 %	≥ 60 min
5	L4	Zero Air	1200	25 ± 1 °C	50 ± 5 %	≥ 60 min

The sensors were exposed to a standard test gas mixture for PID sensor calibration described in ISO 16000-29. The concentration levels selected for this experiment were based on TVOC concentrations reported in https://www.lne.be/sites/default/files/atoms/files/rapport_Clean_Air_0.pdf

Table 18 Components and concentrations of the standard VOC mixture used for testing the TVOC (PID) sensor

Compound	Test level L0, µg/m³	Test level L1, µg/m³	Test level L2, µg/m³	Test level L3, µg/m³	Test level L4, µg/m³
1,2 – Dichlorobenzene	0.0	27.4	54.9	165.4	272.6
n-Decane	0.0	27.4	54.8	165.2	272.3
alfa-Pinene	0.0	25.6	51.2	154.3	254.3
Buthylacetate	0.0	21.9	43.9	132.4	218.2
Methylisobythyl ketone	0.0	18.3	36.6	110.2	181.6
Toluene	0.0	17.2	34.4	103.5	170.7
TVOCs	**0.0**	**137.8**	**275.8**	**831.0**	**1369.7**

For this experiment the 3-min (one measuring cycle of the indoor@box devices) average data from each period of a steady-state temperature and RH in the chamber (usually the last 30 minutes from set of conditions) was considered for this analysis.

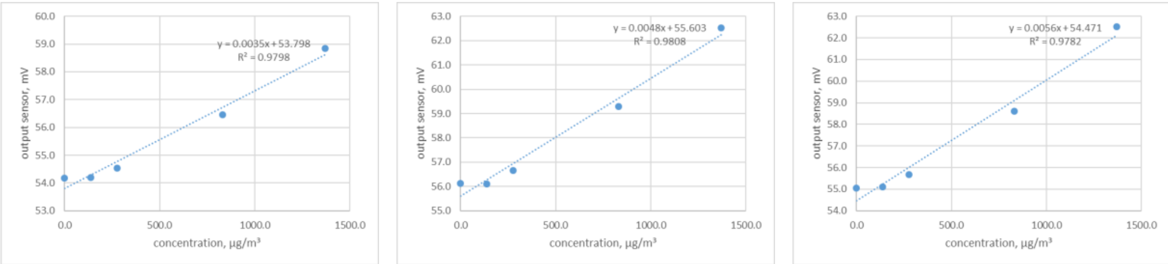

A B C

Figure 28 Graphical presentation of the linear regression analysis of the TVOC sensors of the tested indoor@box devices: B0001 (A); B0002(B) and B0003(C)

Figure 28 shows graphical representations of the linear regressions obtained during the current TVOC (PID) sensor testing. The obtained R^2 linear regression coefficients are shown in Table 16.

Table 19 R^2 linear correlation coefficients of the TVOC (PID) sensors of the tested indoor@box devices

indoor@box ID	TVOC
B0001	0.9798
B0002	0.9808
B0003	0.9782

1.1. INITIAL FIELD TEST

During the initial field test, the available indoor@box monitoring devices were operating simultaneously in the same indoor environment for a pre-defined period (14 days). The overall goal of this test was to compare the outcomes from different indoor@box devices.

1.1.1. Test environment

A single-family dwelling was selected for this initial field test. The test environment was a two-room apartment, located on the 3rd floor of an apartment building. The apartment consists of one bedroom, one bathroom and a living room with open kitchen. The test environment was equipped with mechanical ventilation system type D. The available indoor@box test devices where installed at proximity to each other in a configuration allowing free air movement around the individual devices (Figure 29).

Figure 29 Initial field test configuration

1.1.2. Between-instrument uncertainty

To be able to compare the measurements between the individual indoor@box devices, the concept of relative between-sampler/instrument uncertainty (w_{bs}) was used. The w_{bs} was estimated from the difference of all measurements at pre-defined sampling period (for indoor@box device, the sampling period is every 3 minutes) of the tested samplers/instruments operated in parallel using the following equation (Commission 2010):

$$w_{bs} = \sqrt{\frac{\sum_{i=0}^{n}\left(y_{i,1} - y_{i,2}\right)^2}{2n\bar{y}^2}} \qquad 3$$

where

$y_{i,1}$ and $y_{i,2}$ are the results of parallel measurements for a single measurement period i
n – number of measurement results
$\bar{y}$ – average of all measurement results of the tested devices

Because there is currently no regulatory defined relative between-sampler/instrument uncertainty objective for indoor air quality assessment, the requirements concerning the performance of analytical methods and the interpretation of results (Council Directive 96/23/EC) were used. For the purpose of the performance testing of indoor@box devices, the defined by the directive limit value of 20% relative between instrument uncertainty was used as data quality objective.

1.1.3. Results

The time series of the data for CO_2, temperature, relative humidity and light intensity, and the corresponding orthogonal regressions between the devices, obtained during the initial field tests of the used in this study indoor@box devices are shown in Figure 30.

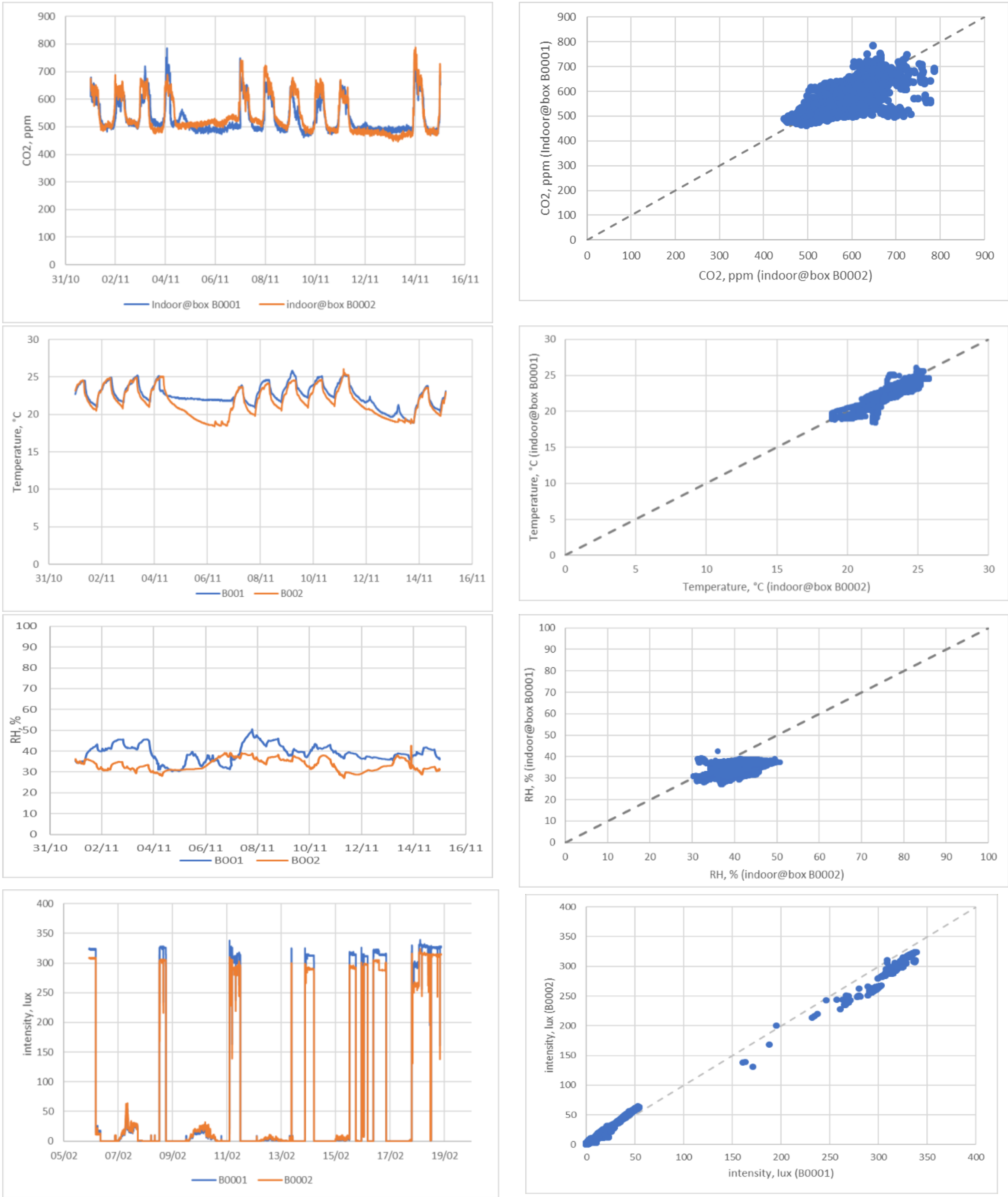

A B

Figure 30 Time series (A) and an orthogonal regression (B) plots of the raw measurements from the tested indoor@box devices during initial field test in the selected indoor test environment.

The estimated between instrument uncertainties (w_{bs}) for CO_2, temperature and RH are shown in Table 20.

Table 20 Resulted relative between instrument uncertainties estimated between the tested indoor@box devices during initial field test.

Parameter	Relative between- instrument uncertainty (w_{bs}), %
Carbon dioxide	5.1
Temperature	4.1
Relative humidity	13.9
Light intensity	5.4

The following plots (Figure 31) show the time series and the corresponding orthogonal regressions of the data for TVOC, NO_2 and CO between the devices, obtained during the indoor@box initial field tests. To be able to compare the outcomes from these sensors without any additional interferences from the calibration process, the evaluation for these parameters were performed using the raw signal from the corresponding sensors.

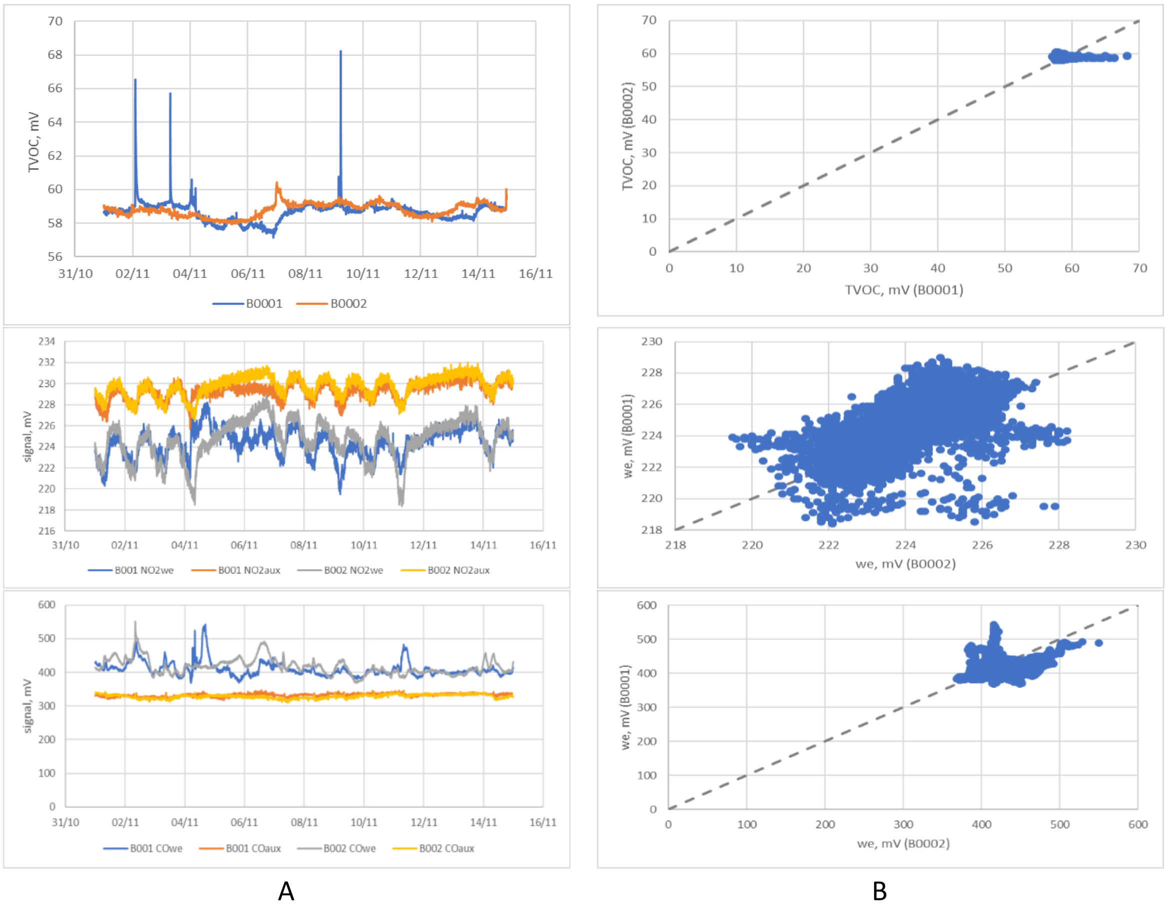

Figure 31 Time series (A) and an orthogonal regression (B) plots of the raw measurements from the tested indoor@box devices during initial field test in the selected indoor test environment.

The resulted between instrument uncertainties for TVOC, NO_2 and CO are shown in Table 21.

Table 21 Resulted relative between instrument uncertainties estimated for NO_2, CO and TVOCs between the tested indoor@box devices during initial field test.

Parameter	Relative between- instrument uncertainty (w_{bs}), %
TVOCs	0.7
NO_2	66.1
CO	34.3

The obtained time series and the corresponding orthogonal regressions of the PM measurements between the tested indoor@box devices are shown in Figure 32.

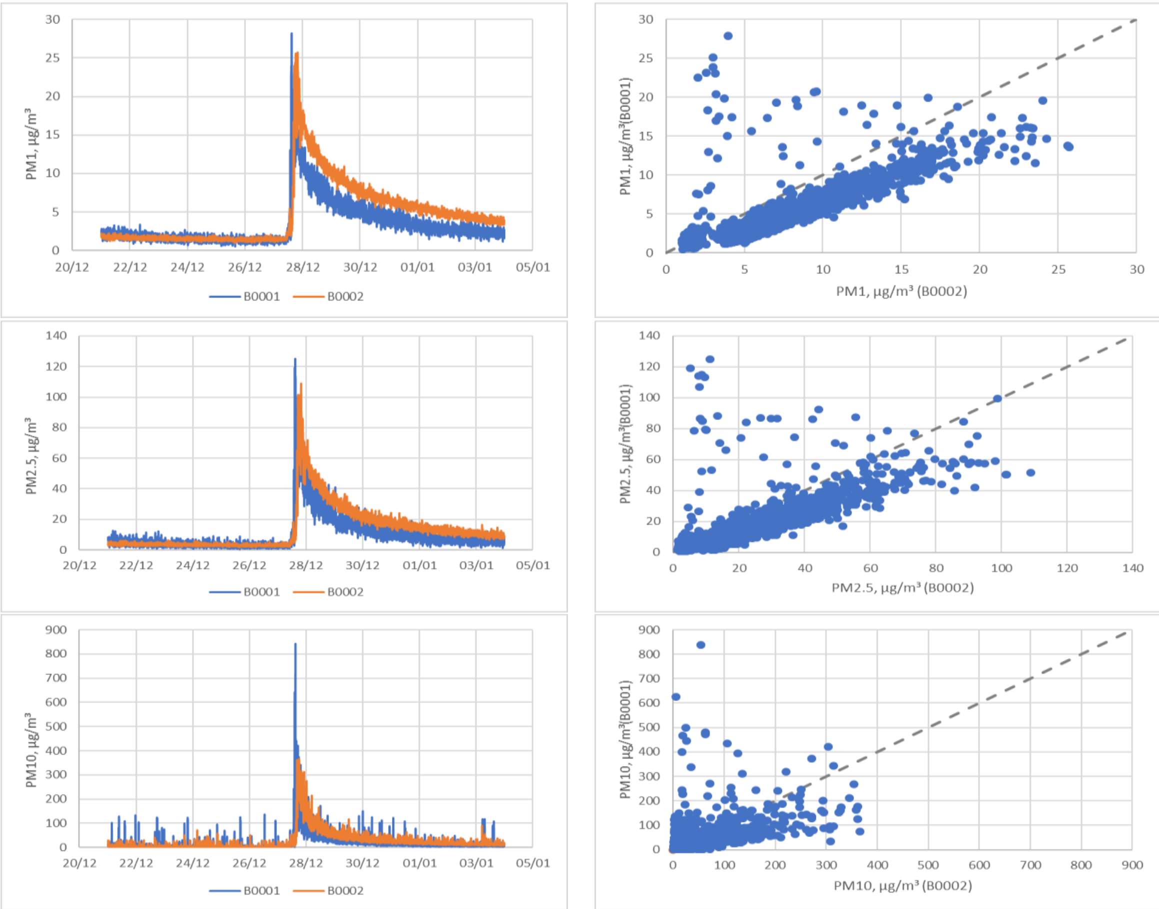

A B

Figure 32 Time series (A) and an orthogonal regression (B) plots of the raw PM measurements from the tested indoor@box devices during initial field test in the selected indoor test environment.

The resulted between instrument uncertainties for different PM fractions are shown in the following table (Table 22).

Table 22 Resulted relative between instrument uncertainties of PM_1, $PM_{2.5}$ and PM_{10} estimated between the tested indoor@box devices during initial field test.

Parameter	Relative between- instrument uncertainty (w_{bs}), %
PM_1	43.4
$PM_{2.5}$	56.7
PM_{10}	119.5

The overall presented time series showed comparable measurements between the tested indoor@box devices during the performed initial field test. However, the relative between-instrument uncertainty estimated for the individual parameters, complies with the pre-defined objective of 20% only for CO_2, T, RH and TVOC.

The higher value of the relative between- instrument uncertainty observed for the NO_2 sensor is most likely caused by interferences and cross sensitivity from other gasses. For instance, several studies showed that the output of the used in this project NO_2 sensor is strongly influenced by the ozone concentrations and the variation in temperature and humidity of the tested environment (Spinelle et al. 2015a, Spinelle et al. 2015b).

The large, relative between- instrument, uncertainty also observed for PM sensors is most probably caused by the large variety in term of PM (Benabed and Limam 2017), of the real occupied indoor environment, where the test conditions cannot be easily controlled. Possible variation in the PM concentrations sampled from each individual indoor@box measuring device is very likely to occur during this test.

1.2. REFERENCE FIELD TESTS

The information obtained during testing gas and PM sensors in laboratory conditions is very helpful for studying the mechanisms and responses of a sensor in various physical and chemical environmental conditions. However, several studies also concluded that the response characteristics observed under laboratory conditions are really reproduced in real environments when the air matrix is more complex and physical conditions are more variable. Furthermore, several authors noted as well that although, the factory calibration is generally sufficient for high concentration (ppm) levels tests in the lab, in real indoor environments and target gas concentrations at ppb levels, more complex methods for obtaining reliable measurements data from the sensors are needed.
Therefore, in this part of the field testing, the indoor@box devices were simultaneously operating together with reference (discontinue) measurement instruments and techniques in the same real indoor environment. The aim of these tests is to evaluate the uncertainty of the linear model (developed during the calibration of the sensors under controlled, laboratory conditions) as well as the error between measurements of indoor@box and the reference instrument for selected parameters under real indoor environmental conditions.

→ Reference measurement techniques

During reference field tests, the target parameters were measured simultaneously with the indoor@box device and reference measurement techniques in the selected indoor environments. A list of all reference devices used during the reference field tests is shown in Table 23.

Table 23: List of reference techniques used during reference field testing of the indoor@box devices

Parameter	Reference monitor/measurement technique	Measurement range	Mode of measurement
PM	Grimm 11-D Optical Particulate Matter monitor	0 - 100 mg/m³	Calibrated for continue PM1, PM2.5 and PM10 mass concentration monitoring
CO_2	Catec Klimabox	0 – 10 000 ppm	Calibrated carbon dioxide monitor based on NDIR sensing technology
Temperature	Catec Klimabox Testo 175-H1 T/RH data logger	-20 to +55°C -20 to +55°C	Continuously Continuously
Relative Humidity	Catec Klimabox Testo 175-H1 T/RH data logger	0 – 100 %RH 0 – 100 %RH	Continuously Continuously
Light intensity	Testo 545	0 to 100 000 lux	Continuously
TVOCs	Radiello passive sampler		Discontinuously (7 days average)

1.2.2. Test environments

The following indoor environments where used to perform the reference field tests. Because of the availability of the reference instruments and the time arrangements with the test locations, different sets of parameters were tested at the different locations.

→ Indoor test environment 1 (Mol)

This indoor test environment was an office room, located in an office building in Mol. The office room is arranged as a landscape office with 10 working stations. The floor of the office was covered with moquette type carpet made from synthetic material. The average occupancy of the office was below 50% during the period of the test.

Figure 33 Reference field test configuration at indoor test environment 1 (Mol)

→ **Indoor test environment 2 (Kraainem)**

This indoor test environment was a single-family dwelling located in Kraainem. The test environment was three rooms apartment, located on the 3th floor of a residence building. The dwelling consists of a living room with open kitchen, a bathroom, a bedroom and an extra room used as an office space. The dwelling was equipped with a central mechanical extraction system only for the toilet and a small storage room, where the gas heating device was located.

→ **Indoor test environment 3 (Eksel)**

The indoor test environment was a single-family dwelling located in Eksel. The test environment was located at the 1st floor of an apartment building and consist of a living room with an open kitchen, a bathroom and a bedroom. The field tests of the indoor@box took place in the living room of the dwelling. The living room was equipped with double glass windows with ventilation grids. The ventilation grids were kept open during the entire field validation test.

→ **Indoor test environment 4 (Keiem)**

This indoor test environment was a single-family dwelling located in Keiem. The test environment was a single house, located in a rural area. The measurements took place in the living room of the house, located on the ground floor.

Figure 34 Reference field test configuration at indoor test environment 4 (Keiem)

→ Indoor test environment 5 (Jonkershove)

This indoor test environment was a single-family dwelling located in Jonkershove. The test environment was a single house, located in a rural area. The measurements took place in the living room of the house, located on the ground floor. There was a biomass burning fireplace installed in the test environment.

Figure 35 Reference field test configuration at indoor test environment 5 (Jonkershove)

→ Indoor test environment 6 (Leke)

This indoor test environment was a single-family dwelling located in Leke. The test environment was a single house, located in a rural area. The closest street was located within 30 m from the house. The inhabitanst reported that the most recent renovations performed in the house took place in 2005 and included replacing the floor and installing a floor insulation. The measurements took place in the living room of the house, located on the ground floor. The total volume of the living room was estimated to be 97 m³. There was a biomass burning fireplace installed in the test environment. The inhabitants reported that the air in the living room have been often refreshed by means of opening the window for more than 15 min every day.

 

Figure 36 Reference field test configuration at indoor test environment 6 (Leke)

→ Indoor test environment 7 (Koekelare)

This indoor test environment was a single-family dwelling located in Koekelare. The test environment was a single house, located in a rural area. The closest street was located within 30 m from the house. The inhabitants reported that there were no major renovations performed in the house for the last two years. The measurements took place in the living room of the house, located on the ground floor. The total volume of the living room was estimated to be 135 m³. The house was equipped with a ventilation system type C with manual control of the flow. There was a biomass burning stove installed in the test environment. The inhabitants reported that the air in the living room have been often refreshed by means of opening the window for more than 15 min every day. There was also a cat, constantly presented in the house during the measurements.

 

Figure 37 Reference field test configuration at indoor test environment 7 (Koekelare)

→ Indoor test environment 8 (Mariakerke)

This indoor test environment was a single-family dwelling located in Mariakerke. The test environment was a single house, located in a rural area. The closest street was located within 5 m from the house. The measurements took place in the living room of the house, located on the ground floor. The total volume of the living room was estimated to be 96 m³. The house was equipped with a ventilation system type C with manual control of the flow. There was a biomass burning stove installed in the test environment. The inhabitants reported that the windows of the living room have been often opened for a long period of time during the day as well as during the night. There were also two cats, constantly present in the house during the measurements.

Figure 38 Reference field test configuration at indoor test environment 8 (Mariakerke)

→ Indoor test environment 9 (Deftinge)

This indoor test environment was a single-family dwelling located in Deftinge. The test environment was half-open house, build in 2010 and located in a rural area. The closest street was located within 30 m from the house. The measurements took place in the living room of the house, located on the ground floor. The total volume of the living room was estimated to be 90 m³. There was a biomass burning stove installed in the test environment. The inhabitants reported that the windows of the living room have been often opened for a long period of time during the day and night.

Figure 39 Reference field test configuration at indoor test environment 9 (Deftinge)

→ Indoor test environment 10 (Schelle)

This indoor test environment was a single-family dwelling located in Schelle. The test environment was a row house, located in an urban environment. The closest street was located within 2 m from the house. The last renovations measures in the house were performed more than a year before the experiment and included painting and a replacement of the biomass burning stove and the chimney. The measurements took place in the living room of the house, located on the ground floor. The inhabitants reported that the air in the living room have been often refreshed by means of opening the window for more than 15 min every day.

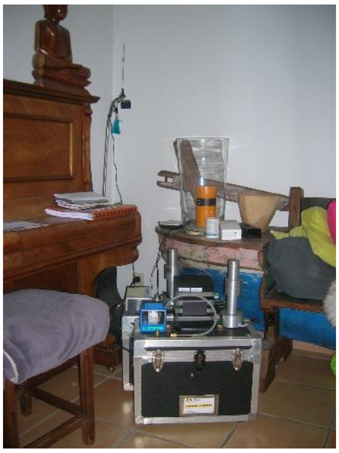

Figure 40 Reference field test configuration at indoor test environment 10 (Schelle)

4.1.6 Compatability of indoor@box measurements with reference methods

To be able to quantify the performance of the measurements from the indoor@box devices, the compatibility of the indoor@box measurement with the reference method was used. The uncertainty resulted due to "lack of comparability" between the indoor@box measurements and the reference method, under real indoor environmental conditions (i.e. field uncertainty), was used as a quantitative indicator to measurement performance of the sensors integrated into the indoor@box devices. The field uncertainty was evaluated assuming linear relationship between measurements obtained from both instruments (indoor@box device (x) and reference instrument (Y)) following the model described in eq. *4*, using an orthogonal regression (eq. *5* - *9*) (Commission 2010, Spinelle et al. 2013).

$$Y_i = a + bx_i \qquad (4)$$

where

- Y_i are the N sensor responses
- x_i are the measurements by the reference measurement technique
- a is the intercept of an orthogonal regression
- b is the slope of an orthogonal regression

The orthogonal regression was carried out using the following set of equations (Commission 2010):

$$S_{xx} = \sum_{i=1}^{N} (x_i - \bar{x})^2 \qquad (5)$$

$$S_{YY} = \sum_{i=1}^{N} (Y_i - \bar{Y})^2 \qquad (6)$$

$$S_{Yx} = \sum_{i=1}^{N} (x_i - \bar{x})(Y_i - \bar{Y}) \qquad (7)$$

$$\bar{x} = N^{-1} \sum_{i=1}^{N} x_i \qquad (8)$$

$$\bar{Y} = N^{-1} \sum_{i=1}^{N} Y_i \qquad (9)$$

The intercept (a) and slope (b) of the regression is determined by (Commission 2010):

$$b = \frac{S_{YY} - S_{xx} + \sqrt{(S_{YY} - S_{xx})^2 + 4S_{Yx}^2}}{2S_{Yx}} \qquad (10)$$

$$a = \bar{Y} - b\bar{x} \qquad 11$$

RSS represents the sum of the residuals from the orthogonal regression:

$$RSS = \sum_{i=1}^{N}(Y_i - a - bx_i)^2 \text{ when } (Y_i - a - bx_i)^2 \text{ is constant} \qquad 12$$

$$RSS = (a + bx_i)^2 \sum_{i=1}^{N}\left(\frac{Y_i}{a+bx_i} - 1\right)^2 \text{ when } \left(\frac{Y_i}{a+bx_i} - 1\right)^2 \text{is constant} \qquad 13$$

The uncertainty due to lack of compatibility with the reference method, (u_{CR}), was then calculated as:

$$u_{CR} = \left|\sqrt{\frac{RSS}{n-2} - u(x_i)^2 + (a + (b-1)x_i)^2}\right| \qquad 14$$

where

u(x_i) is the random uncertainty of the reference method (Commission 2010)

The combined relative field uncertainty for the evaluated parameter $w_{CM,field}$ was then calculated, taking as Y_i the concentration at the limit value:

$$w_{CM,field}(Y_i) = \sqrt{\frac{U_{CR}^2}{Y_i^2}} \qquad 15$$

For each of the datasets the expanded relative uncertainty of the results of the tested method (sensor) was also calculated, by multiplying $w_{CM,field}$ by a specified coverage factor k reflecting the appropriate number of degrees of freedom resulting from the determination of $w_{CM,field}$ as:

$$W_{CM,field} = k \cdot w_{CM,field} \qquad 16$$

In view of large number of data available, a coverage factor of k=2 can be used (Commission 2010).

The initially developed models, defined under laboratory conditions for each of the used sensors (i.e. laboratory sensor calibration models) were applied to the outcomes from the indoor@box devices to get the corrected (according to the lab calibration model) sensors' response during the field tests.
Because there are currently no available specified data quality objectives regarding the indoor air quality assessment measurements, the obtained during these field tests relative uncertainties were compared with the data quality objectives for indicative measurements of ambient air quality assessment for the corresponding parameters defined in EU directive 2008/50/EC (Parliament 2008).

4.1.7 Results

4.1.7.1 Particulate matter

The time series of the data obtained from the indoor@box and reference monitor (Grimm), during the reference field tests for PM are shown in Figure 41. The values from the indoor@box presented in these plots have been corrected regarding the linear regression model obtained during the calibration process of the PM sensor under laboratory conditions.

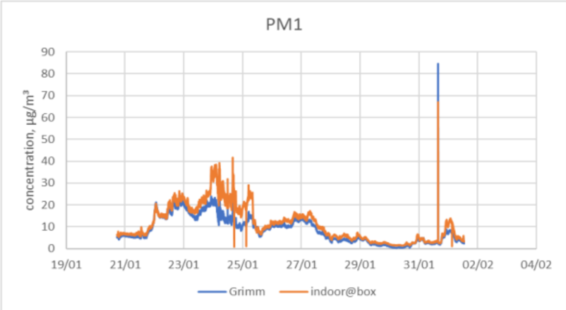

A

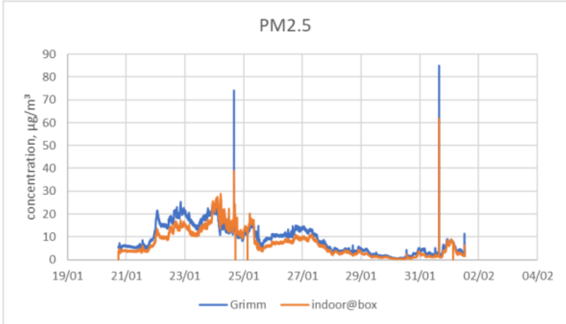

B

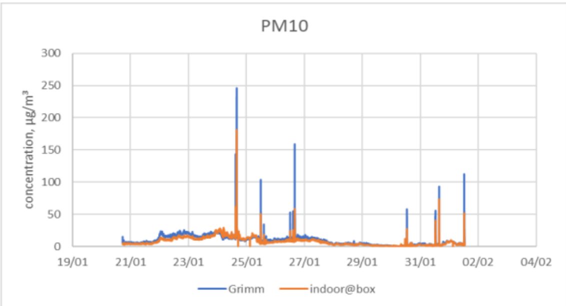

C

Figure 41 Time series of data obtained from indoor@box and reference PM monitor (Grimm) for PM_1 (A), $PM_{2.5}$ (B) and PM_{10} (C) fractions, during reference field test at indoor test location 1 (Mol) after .....

The orthogonal regression plots of the indoor@box and reference PM monitor (Grimm) measurements from the lab calibration and reference field test are shown in Figure 42.
The resulted combined and expanded relative uncertainty of the compatibility of the measurements obtained from the indoor@box device with the reference PM monitor (Grimm) for the different PM fractions are shown in Table 24.

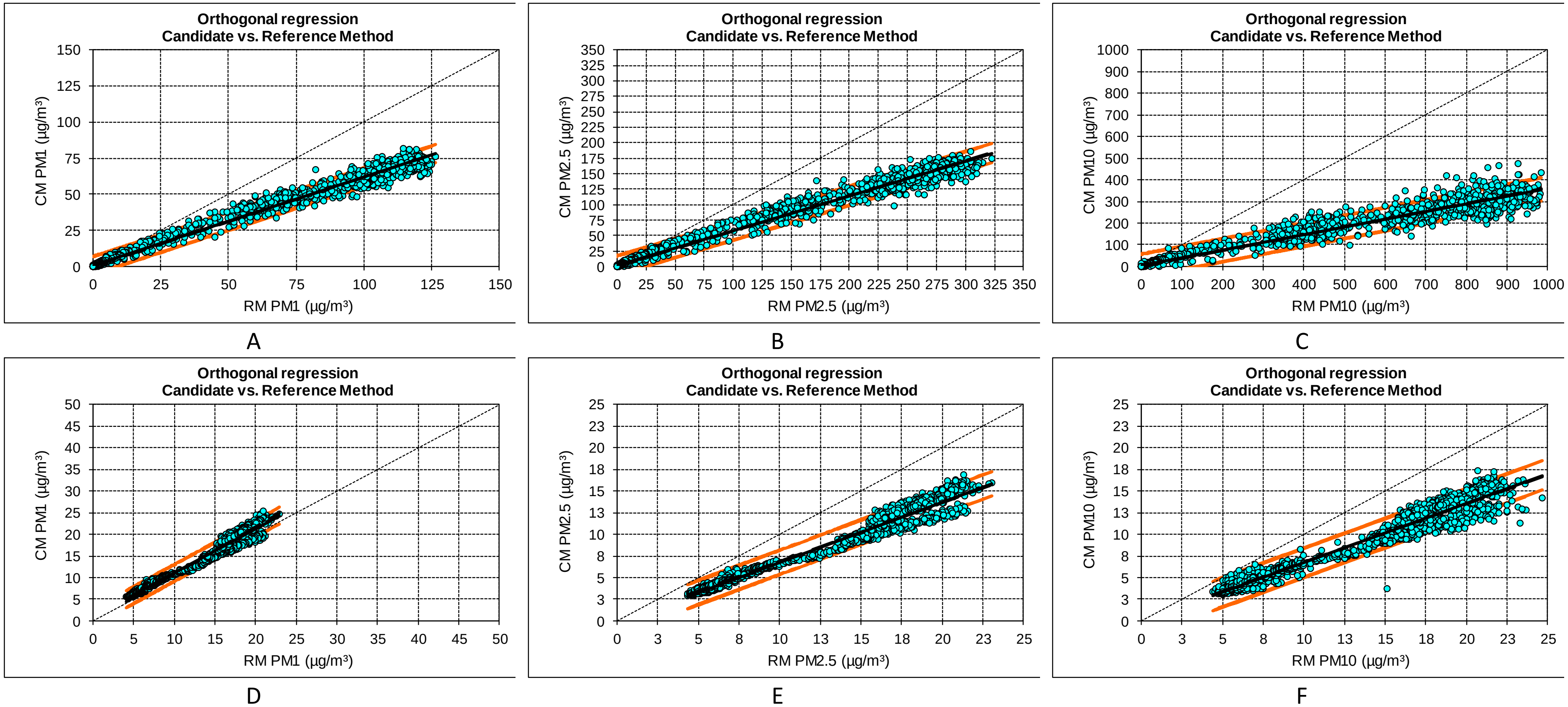

Figure 42 Orthogonal regression plots of the measurements from the reference PM monitor (RM) and indoor@box (CM) during verification in controlled (lab) conditions (A: PM_1; B: $PM_{2.5}$, C: PM_{10}) and during reference field test in real indoor environment (D: PM_1; E: $PM_{2.5}$; F: PM_{10})

Table 24: Uncertainty from the reference field test of indoor@box. The measurements of the indoor@box were corrected regarding the linear model estimated during lab calibration.

	PM_1	$PM_{2.5}$	PM_{10}
Combined uncertainty, µg/m³	1.6	7.8	15.8
Combined relative uncertainty at the limit value ($w_{CM,field}$), %	6.4[a]	31.1[a]	31.5[b]
Expanded relative uncertainty at the limit value ($W_{CM,field}$), %	12.4[a]	62.1[a]	63.4[b]

[a] limit value of 25µg/m³ was used (Directive 2008/50/EU)
[b] limit value of 50 µg/m³ was used (Directive 2008/50/EU)

The overall combined relative uncertainty, estimated for all PM fractions at the corresponding limit values were lower than the maximal defined standard uncertainty (i.e. 50% defined in Directive 2008/50/EC (Parliament 2008)) of an indicative measurement techniques. The expanded relative uncertainty, however, complies with the requirements only for PM_1 fraction and it shows slightly higher values for $PM_{2.5}$ and PM_{10}.
To try to lower the relative uncertainty of the PM measurements of the indoor@box device, the method of field calibration was applied additionally during this experiment.
In general, the field calibration method, uses the measurements from the indoor@box PM sensor and outcomes from the reference PM monitor (Grimm) to establish a new linear model (field calibration model) which then is used, instead of the laboratory calibration model, to correct the measurements from the indoor@box according to the reference value.
The resulted orthogonal regression plots of the measurements from the reference PM monitor and the corrected (according to the field calibration model) measurements from indoor@box device during the reference field test are shown in Figure 43.

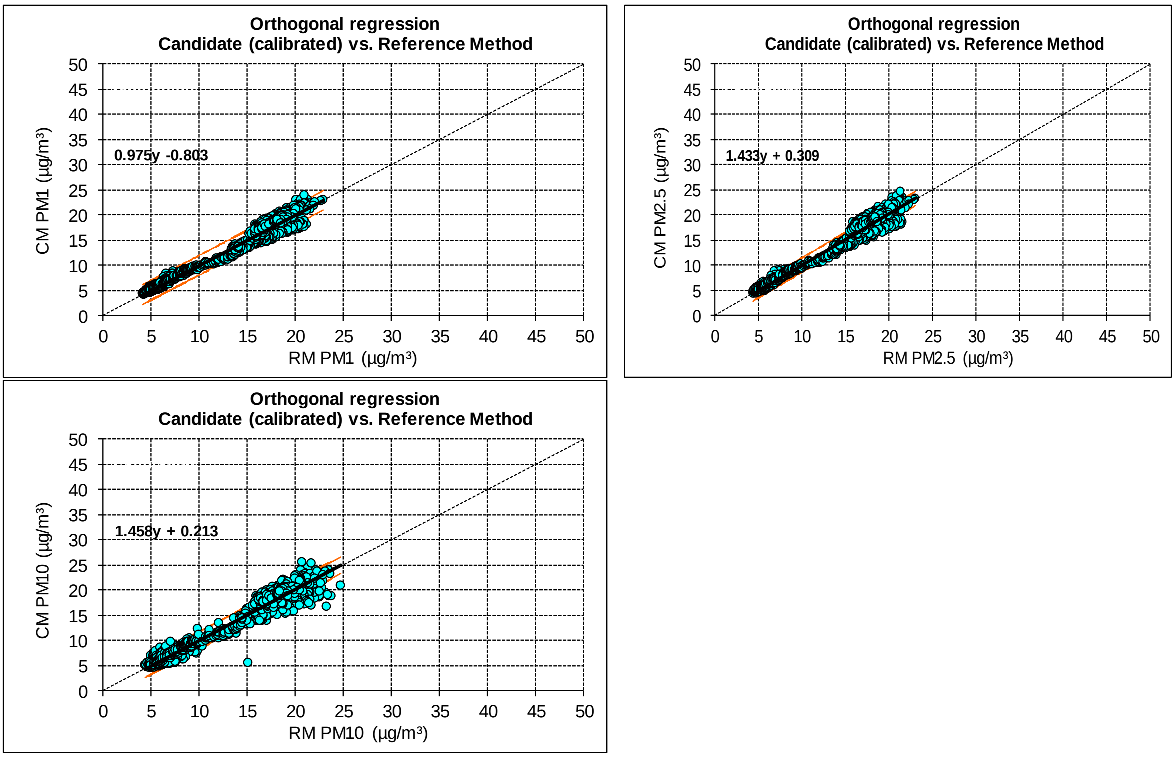

Figure 43 Orthogonal regression plots of the reference PM monitor measurements (RM) and the corrected (according to the field calibration model) indoor@box outcomes (CM) during reference field test in indoor test environment 1 (Mol).

The resulted combined and expanded relative uncertainty of the compatibility of the measurements obtained from the indoor@box device (after correction according to the established field calibration model) with the reference PM monitor (Grimm) for the different PM fractions are shown in Table 25.

Table 25 Uncertainty from the reference field test of indoor@box . The measurements of the indoor@box were corrected according the estimated field calibration linear model.

	PM_1	$PM_{2.5}$	PM_{10}
Combined uncertainty (u_{CR}), µg/m³	0.52	0.65	1.06
Combined relative uncertainty at the limit value ($w_{CM,field}$), %	2.1[a]	2.6[a]	2.2[b]
Expanded relative uncertainty at the limit value ($W_{CM,field}$), %	4.1[a]	5.2[a]	4.3[b]

[a] limit value of 25µg/m³ was used (Directive 2008/50/EU)
[b] limit value of 50 µg/m³ was used (Directive 2008/50/EU)

The outcomes from this additional test showed that the method of establishing a new (field calibration) linear model for correcting the outcomes from the PM sensor used in the tested indoor@box device could be successfully used to reduce the overall relative uncertainty of the performed field measurements. Despite its usefulness, the field calibration model is valid and will be limited only to the monitoring environment, where the field calibration model was established. Moreover, the duration of field calibration need to be such that the variations of the influencing parameters are the same range than during the later implementation of the measurement device (Commission 2010, Spinelle et al. 2013).

4.1.7.2 Carbon dioxide

The results from the reference field tests for carbon dioxide at different test environments are shown below. The values from the indoor@box devices presented in these plots have been corrected regarding the linear regression model obtained during the calibration process of the CO_2 sensor under laboratory conditions.

4.1.7.2.1 Indoor test environment 2 (Kraainem)

The time series and the orthogonal regression plot of the measurement from the indoor@box devices and reference monitor (Catec), during the reference field test at indoor test environment 2 (Kraainem) for CO_2 are shown in Figure 44.

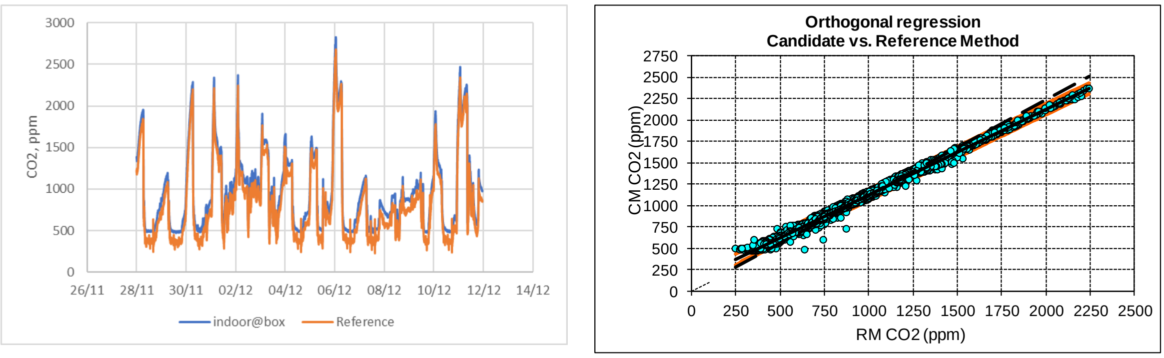

A B

Figure 44 Time series (A) and an orthogonal regression plot (B) of the measurements from the reference CO_2 monitor (RM) and indoor@box (CM) during reference field test in indoor test environment 2 (Kraainem).

The resulted combined and expanded relative uncertainty of the compatibility of the measurements obtained from the indoor@box device with the reference CO_2 monitor (Catec) for defined limit value of 1000 ppm are shown in Table 26.

Table 26 Estimated uncertainties from the CO_2 reference field test of indoor@box . The measurements of the indoor@box were corrected regarding the linear model estimated during lab calibration.

	Carbon dioxide
Combined uncertainty (u_{CR}), ppm	129
Combined relative uncertainty at limit value of 1000 ppm ($w_{CM,field}$), %	12.9
Expanded relative uncertainty at limit value of 1000 ppm ($W_{CM,field}$), %	22.3

4.1.7.2.2 Indoor test environment 4 (Keiem)

Figure 45 shows the time series and the orthogonal regression plot of the measurement from the indoor@box devices and reference monitor (Catec), during the reference field test at indoor test environment 4 (Keiem).

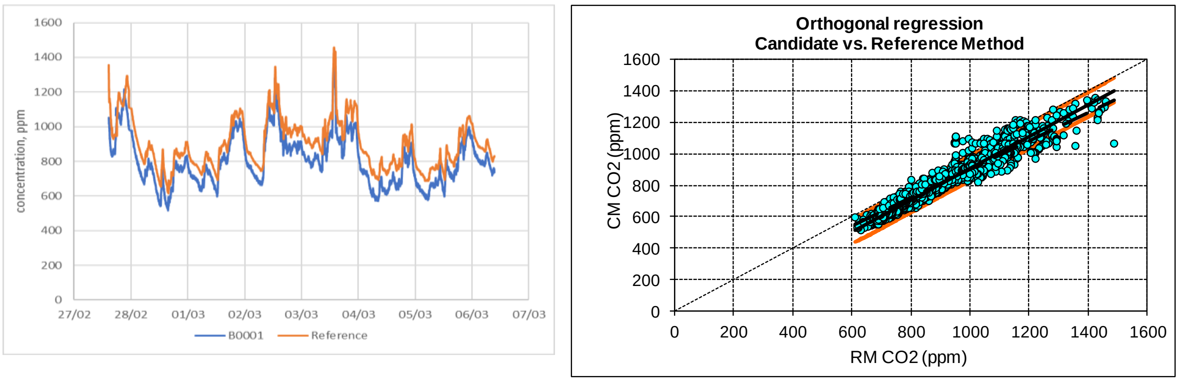

A B

Figure 45 Time series (A) and an orthogonal regression plot (B) of the measurements from the reference CO_2 monitor (RM) and indoor@box (CM) during reference field test in indoor test environment 4 (Keiem).

The resulted combined and expanded relative uncertainty of the compatibility of the measurements obtained from the indoor@box device with the reference CO_2 monitor (Catec) for defined limit value of 1000 ppm are shown in Table 27.

Table 27 Estimated uncertainties from the CO_2 reference field test of indoor@box. The measurements of the indoor@box were corrected regarding the linear model estimated during lab calibration.

	Carbon dioxide
Combined uncertainty (u_{CR}), ppm	97.5
Combined relative uncertainty at limit value of 1000 ppm ($w_{CM,field}$), %	9.8
Expanded relative uncertainty at limit value of 1000 ppm ($W_{CM,field}$), %	19.5

4.1.7.2.3 Indoor test environment 5 (Jonkershove)

Figure 46 shows the time series and the orthogonal regression plot of the measurement from the indoor@box devices and reference monitor (Catec), during the reference field test at indoor test environment 5 (Jonkershove).

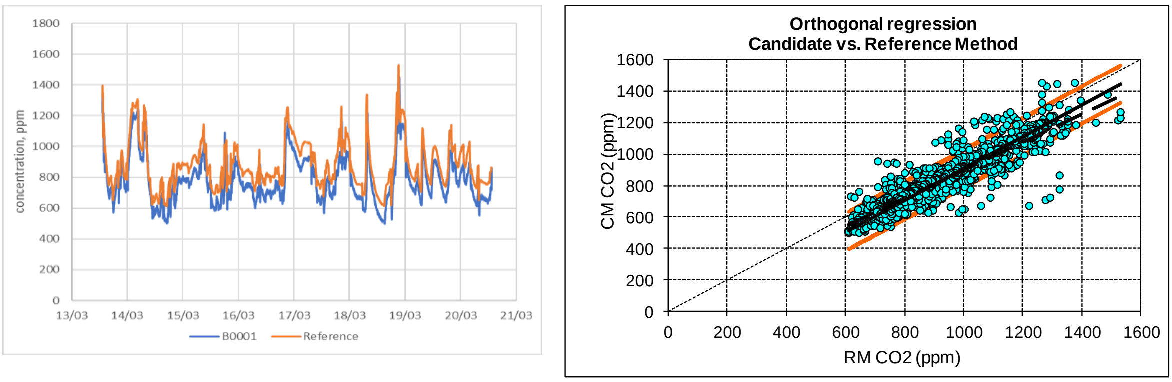

A B

Figure 46 Time series (A) and an orthogonal regression plot (B) of the measurements from the reference CO_2 monitor (RM) and indoor@box (CM) during reference field test in indoor test environment 5 (Jonkershove).

The resulted combined and expanded relative uncertainty of the compatibility of the measurements obtained from the indoor@box device with the reference CO_2 monitor (Catec) for defined limit value of 1000 ppm are shown in Table 28.

Table 28 Estimated uncertainties from the CO_2 reference field test of indoor@box . The measurements of the indoor@box were corrected regarding the linear model estimated during lab calibration.

	Carbon dioxide
Combined uncertainty (u_{CR}), ppm	107
Combined relative uncertainty at limit value of 1000 ppm ($w_{CM,field}$), %	10.7
Expanded relative uncertainty at limit value of 1000 ppm ($W_{CM,field}$), %	21.4

4.1.7.2.4 Indoor test environment 6 (Leke)

Figure 47 shows the time series and the orthogonal regression plot of the measurement from the indoor@box devices and reference monitor (Catec), during the reference field test at indoor test environment 6 (Leke).

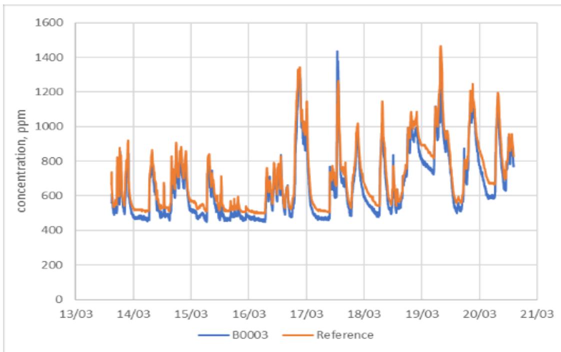

A

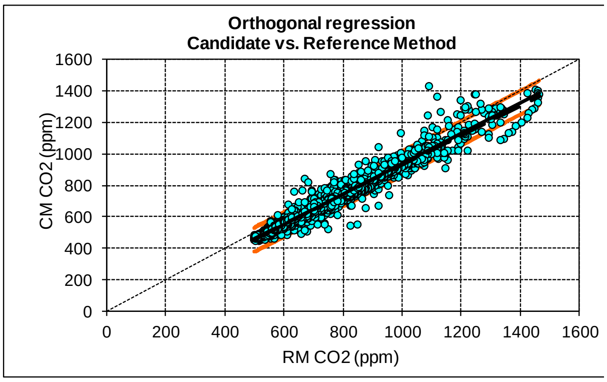

B

Figure 47 Time series (A) and an orthogonal regression plot (B) of the measurements from the reference CO_2 monitor (RM) and indoor@box (CM) during reference field test in indoor test environment 6 (Leke).

The resulted combined and expanded relative uncertainty of the compatibility of the measurements obtained from the indoor@box device with the reference CO_2 monitor (Catec) for defined limit value of 1000 ppm are shown in Table 29

Table 29 Estimated uncertainties from the CO_2 reference field test of indoor@box . The measurements of the indoor@box were corrected regarding the linear model estimated during lab calibration.

	Carbon dioxide
Combined uncertainty (u_{CR}), ppm	70.3
Combined relative uncertainty at limit value of 1000 ppm ($w_{CM,field}$), %	7.0
Expanded relative uncertainty at limit value of 1000 ppm ($W_{CM,field}$), %	14.1

4.1.7.2.5 Indoor test environment 7 (Koekelare)

The time series and the orthogonal regression plot of the measurement from the indoor@box devices and reference monitor (Catec), during the reference field test at indoor test environment 7 (Koekelare) are presented in Figure 48.

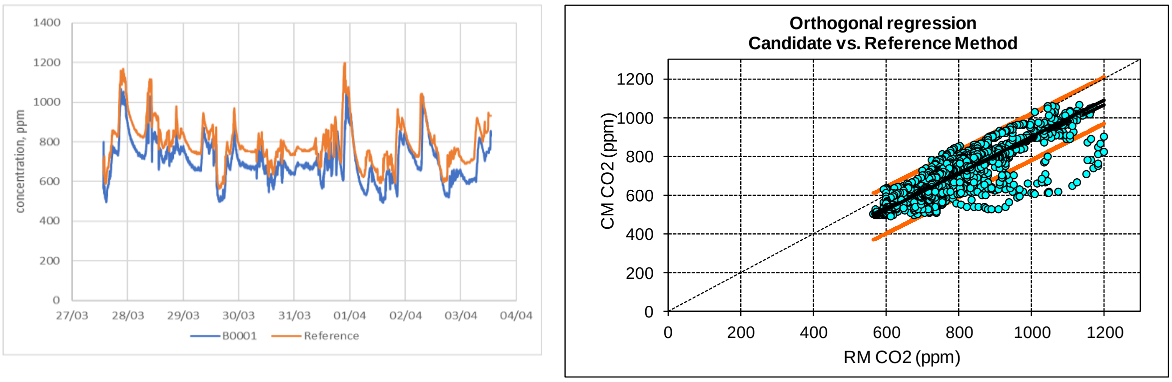

A B

Figure 48 Time series (A) and an orthogonal regression plot (B) of the measurements from the reference CO_2 monitor (RM) and indoor@box (CM) during reference field test in indoor test environment 7 (Koekelare).

The resulted combined and expanded relative uncertainty of the compatibility of the measurements obtained from the indoor@box device with the reference CO_2 monitor (Catec) for defined limit value of 1000 ppm are shown in Table 30.

Table 30 Estimated uncertainties from the CO_2 reference field test of indoor@box . The measurements of the indoor@box were corrected regarding the linear model estimated during lab calibration.

	Carbon dioxide
Combined uncertainty (u_{CR}), ppm	112
Combined relative uncertainty at limit value of 1000 ppm ($w_{CM,field}$), %	11.2
Expanded relative uncertainty at limit value of 1000 ppm ($W_{CM,field}$), %	22.5

4.1.7.2.6 Indoor test environment 8 (Mariakerke)

The time series and the orthogonal regression plot of the measurement from the indoor@box devices and reference monitor (Catec), during the reference field test at indoor test environment 8 (Mariakerke) are presented in Figure 49.

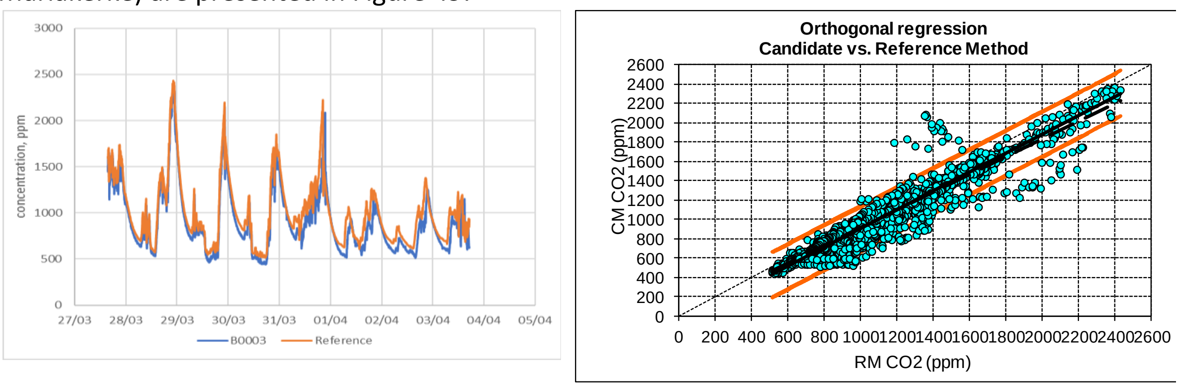

A B

Figure 49 Time series (A) and an orthogonal regression plot (B) of the measurements from the reference CO_2 monitor (RM) and indoor@box (CM) during reference field test in indoor test environment 8 (Mariakerke).

The resulted combined and expanded relative uncertainty of the compatibility of the measurements obtained from the indoor@box device with the reference CO_2 monitor (Catec) for defined limit value of 1000 ppm are shown in Table 31.Table 29

Table 31 Estimated uncertainties from the CO_2 reference field test of indoor@box . The measurements of the indoor@box were corrected regarding the linear model estimated during lab calibration.

	Carbon dioxide
Combined uncertainty (u_{CR}), ppm	142.2
Combined relative uncertainty at limit value of 1000 ppm ($w_{CM,field}$), %	14.2
Expanded relative uncertainty at limit value of 1000 ppm ($W_{CM,field}$), %	28.4

4.1.7.2.7 Indoor test environment 9 (Deftinge)

The outcomes of the measurements from the indoor@box devices and reference monitor (Catec), during the reference field test at indoor test environment 9 (Deftinge) are shown in Figure 50, as time series and orthogonal regression plot.

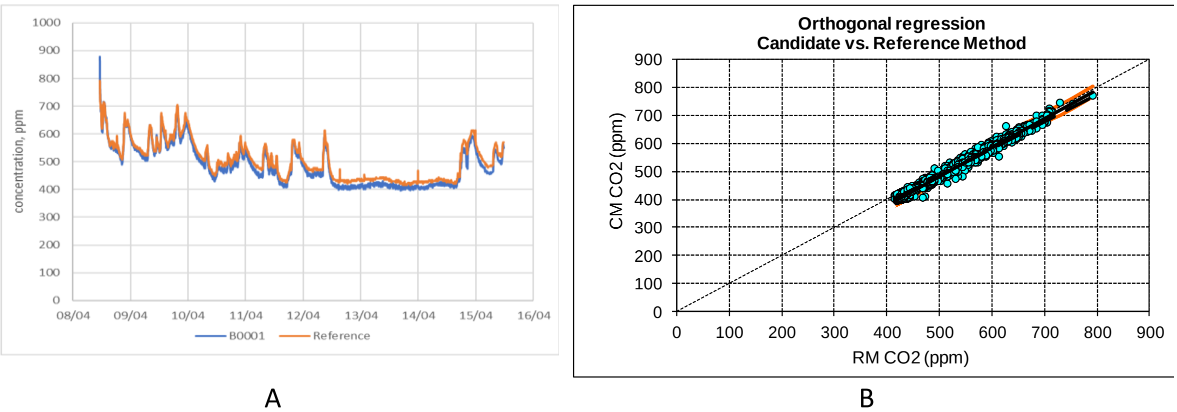

Figure 50 Time series (A) and an orthogonal regression plot (B) of the measurements from the reference CO_2 monitor (RM) and indoor@box (CM) during reference field test in indoor test environment 9 (Deftinge).

The resulted combined and expanded relative uncertainty of the compatibility of the measurements obtained from the indoor@box device with the reference CO_2 monitor (Catec) for defined limit value of 1000 ppm are shown in Table 32Table 29

Table 32 Estimated uncertainties from the CO_2 reference field test of indoor@box . The measurements of the indoor@box were corrected regarding the linear model estimated during lab calibration.

	Carbon dioxide
Combined uncertainty (u_{CR}), ppm	8.2
Combined relative uncertainty at limit value of 1000 ppm ($w_{CM,field}$), %	0.8
Expanded relative uncertainty at limit value of 1000 ppm ($W_{CM,field}$), %	1.6

4.1.7.2.8 Indoor test environment 10 (Schelle)

Figure 51 shows the time series and orthogonal regression plot outcomes of the measurements from the indoor@box device and reference monitor (Catec), during the reference field test at indoor test environment 10 (Schelle).

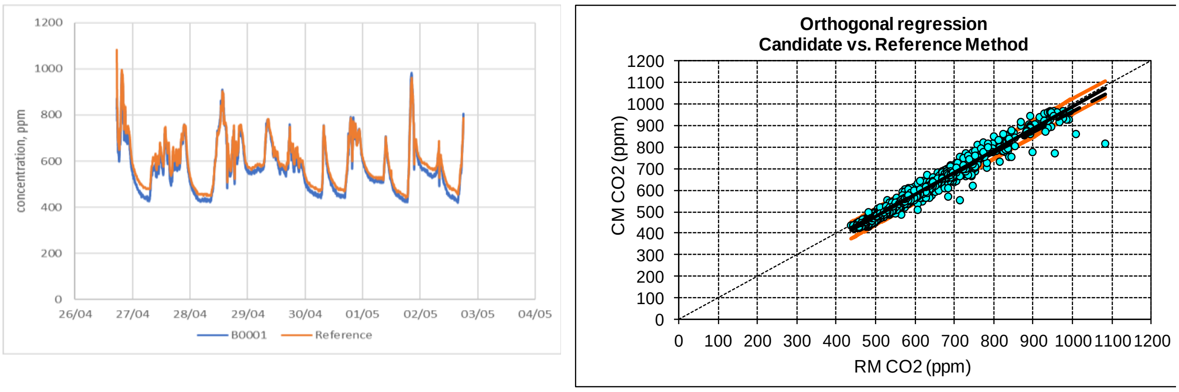

A B

Figure 51 Time series (A) and an orthogonal regression plot (B) of the measurements from the reference CO_2 monitor (RM) and indoor@box (CM) during reference field test in indoor test environment 10 (Schelle).

The resulted combined and expanded relative uncertainty of the compatibility of the measurements obtained from the indoor@box device with the reference CO_2 monitor (Catec) for defined limit value of 1000 ppm are shown in Table 33.Table 29

Table 33 Estimated uncertainties from the CO_2 reference field test of indoor@box. The measurements of the indoor@box were corrected regarding the linear model estimated during lab calibration.

	Carbon dioxide
Combined uncertainty (u_{CR}), ppm	20.8
Combined relative uncertainty at limit value of 1000 ppm ($w_{CM,field}$), %	2.1
Expanded relative uncertainty at limit value of 1000 ppm ($W_{CM,field}$), %	4.2

Although, there is no current requirements regarding the uncertainties of the CO_2 measurements, the obtained combined and extended relative uncertainties of the tested indoor@box devices estimated at limit value of 1000 ppm were within the maximal allowed uncertainty of 30% for indicative measurements of inorganic gasses (e.g. nitrogen dioxide, sulphur dioxide, carbon monoxide) in ambient air quality assessments (Directive 2008/50/EC (Parliament 2008)).

4.1.7.3 Temperature and relative humidity

The results from the reference field tests for temperature and relative humidity at different indoor test environments are shown below. The measurements from the indoor@box devices shown in these plots have been corrected regarding the linear regression model obtained during the calibration process under laboratory conditions.

4.1.7.3.1 Indoor test environment 2 (Kraainem)

The time series and the orthogonal regression plots of the data from the indoor@box and reference monitor (Catec), during the reference field tests for Temperature and RH are shown in Figure 52. The values from the indoor@box presented in these plots have been corrected regarding the linear regression model obtained during the calibration process of the temperature and RH sensors under laboratory conditions.

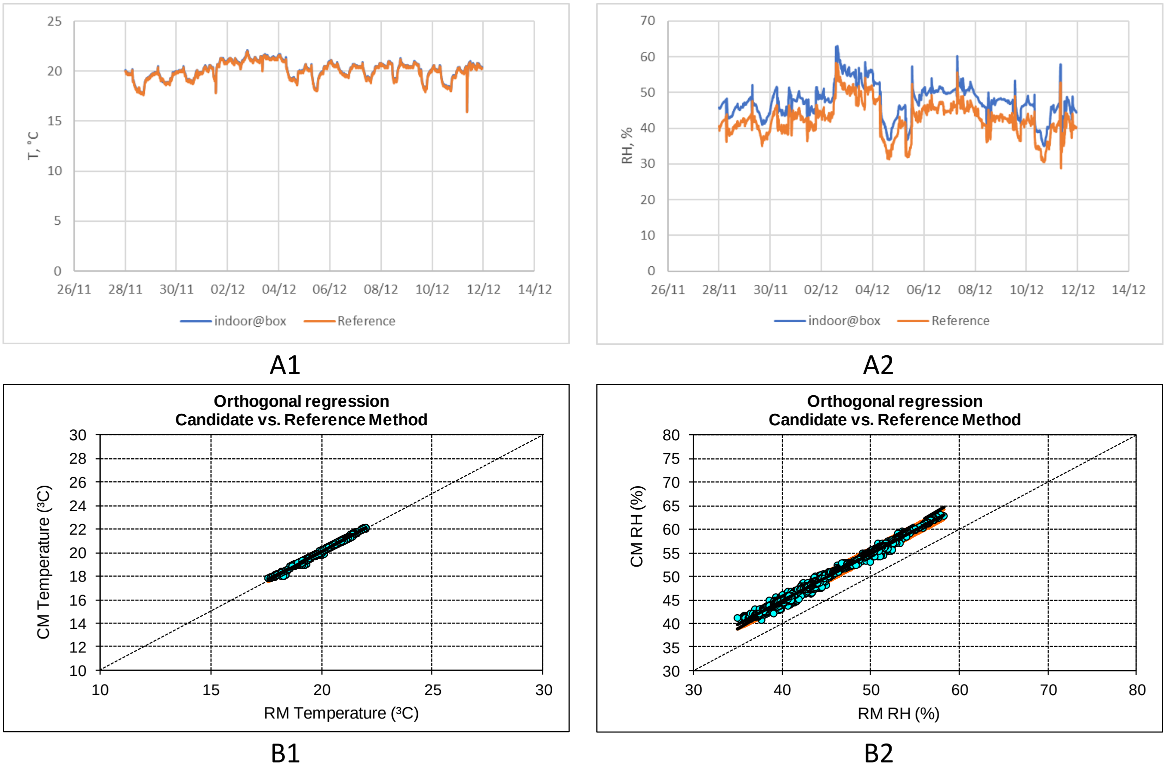

Figure 52 Time series of measured temperature (A1) and RH (A2), together with the corresponding orthogonal regression plots (temperature (B1) and RH (B2) from the reference temperature and RH monitor (RM) and indoor@box (CM) during reference field test in indoor test environment 2 (Kraainem).

The resulted combined relative uncertainty of the compatibility of the measurements obtained from the indoor@box device with the reference T/RH monitor (Catec) is shown in Table 34.

Table 34 Estimated uncertainties from the T and RH reference field tests of indoor@box. The measurements of the indoor@box were corrected regarding the linear model estimated during lab calibration.

	Temperature	RH
Combined uncertainty (u_{CR})	0.2 °C	4.9 %

4.1.7.4 Total Organic Hydrocarbons

The outcomes from the reference field tests of the TVOC sensor of the indoor@box devices at different test environments are shown below. The TVOC concentrations from the indoor@box devices presented in the following plots have been corrected according to the linear regression models obtained during the calibration process of the TVOC sensors in laboratory conditions. The reference measurement technique for TVOC used during these field tests was a discontinues measurement using passive sampler (Radiello) followed by GC-MS analysis, resulting to an average value of TVOCs over the defined sampling period (typically 7 days). To be able to compare the results, between the continues measurements of indoor@box and the weekly average from the reference method (Radiello), a comparison between the average measurements for the same sampling period was performed.

4.1.7.4.1 Indoor test environment 3 (Eksel)

The time series of the measurements from the indoor@box during the reference field test are shown in Figure 53.

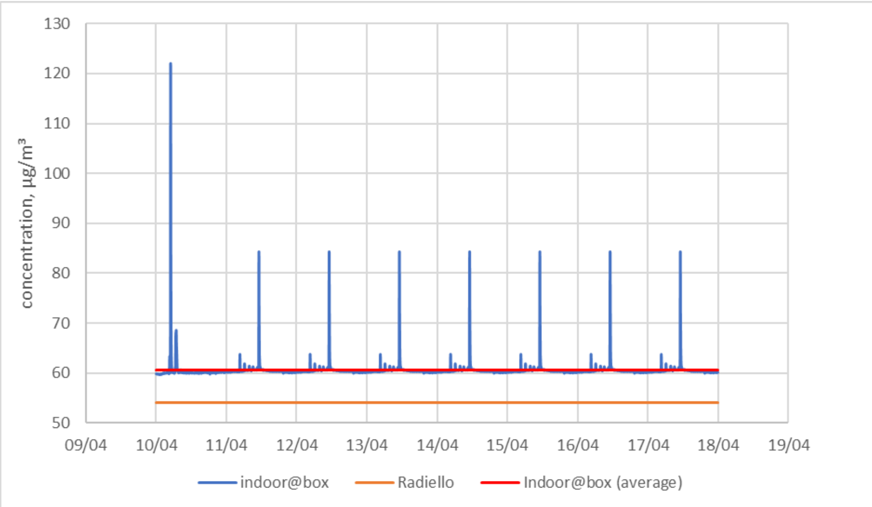

Figure 53 Time series of data obtained from indoor@box and reference measurement technique (Radiello) for TVOCs, during reference field test at indoor test location 3 (Eksel)

The resulted average TVOC concentrations and the estimated relative difference between the indoor@box and the reference method (Radiello) from the reference field test are shown Table 35.

Table 35 Resulted TVOC concentrations and the estimated relative difference obtained during the reference field test at indoor test environment 3 (Eksel)

	Radiello	indoor@box
Sampling period	7 days (10/04 – 18/04)	7 days (10/04 – 18/04)
TVOCs (average), µg/m³	54 µg/m³	61 ± 2 µg/m³
Relative difference between the TVOCs averages measured by the reference technique (Radiello) and indoor@box	12.3%	

4.1.7.4.2 Indoor test environment 4 (Keiem)

The time series of the measurements from the indoor@box during the reference field test at indoor test environment 4 are shown in Figure 54.

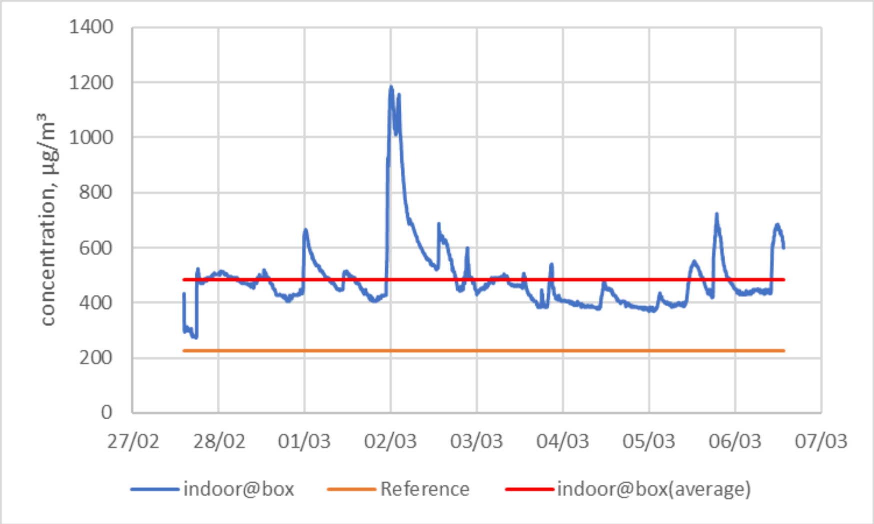

Figure 54 Time series of data obtained from indoor@box and reference measurement technique (Radiello) for TVOCs, during reference field test at indoor test location 4 (Keiem)

The resulted average TVOC concentrations and the estimated relative difference between the indoor@box and the reference method (Radiello) from the reference field test performed at indoor test location 4 are shown Table 36.

Table 36 Resulted TVOC concentrations and the estimated relative difference obtained during the reference field test at indoor test environment 4 (Keiem)

	Radiello	indoor@box
Sampling period	7 days (27/02 – 06/03)	7 days (27/02 – 06/03)
TVOCs (average), µg/m³	224 µg/m³	483 ± 124 µg/m³
Relative difference between the TVOCs averages measured by the reference technique (Radiello) and indoor@box	115%	

4.1.7.4.3 Indoor test environment 5 (Jonkershove)

The time series of the measurements from the indoor@box during the reference field test performed at indoor test environment 5 are shown in Figure 55.

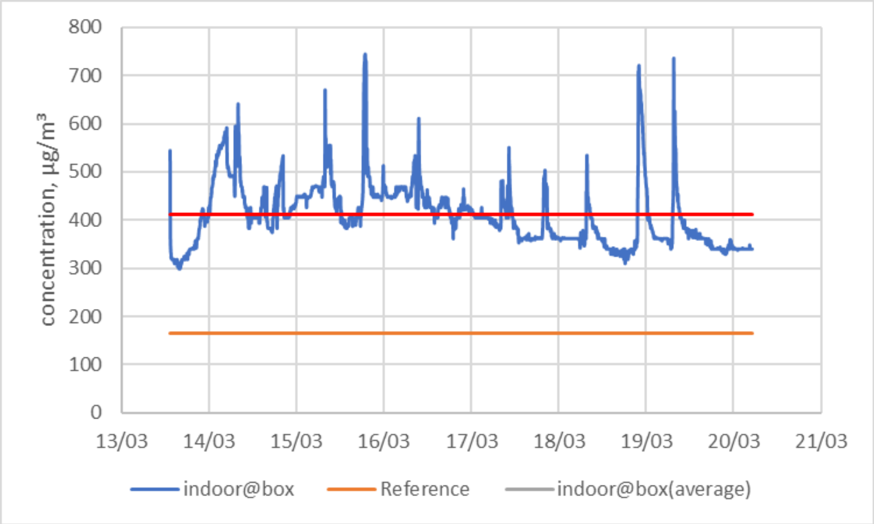

Figure 55 Time series of data obtained from indoor@box and reference measurement technique (Radiello) for TVOCs, during reference field test at indoor test location 5 (Jonkershove)

The resulted average TVOC concentrations and the estimated relative difference between the indoor@box and the reference method (Radiello) from the reference field test performed at indoor test location 5 are shown Table 37Table 36.

Table 37 Resulted TVOC concentrations and the estimated relative difference obtained during the reference field test

	Radiello	indoor@box
Sampling period	7 days (13/03 – 20/03)	7 days (13/03 – 20/03)
TVOCs (average), µg/m³	165 µg/m³	411 ± 66 µg/m³
Relative difference between the TVOCs averages measured by the reference technique (Radiello) and indoor@box	115%	

4.1.7.4.4 Indoor test environment 6 (Leke)

The time series of the measurements from the indoor@box during the reference field test are shown in Figure 56.

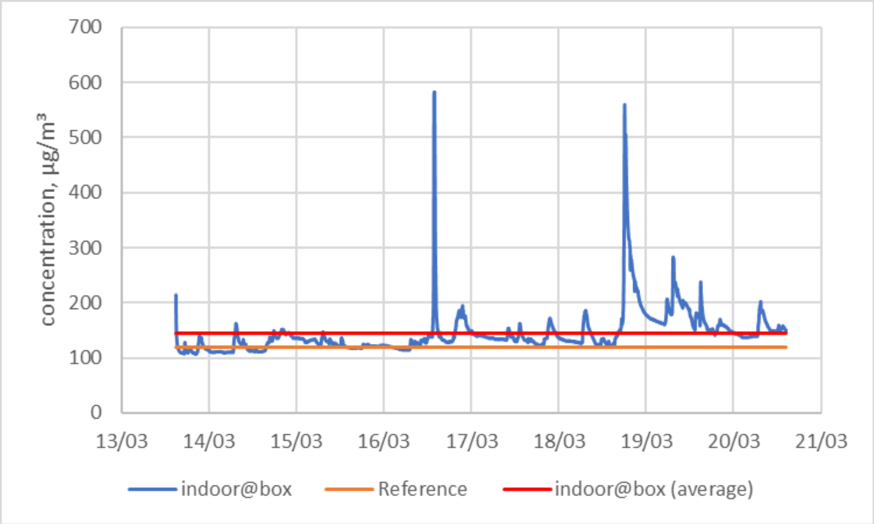

Figure 56 Time series of data obtained from indoor@box and reference measurement technique (Radiello) for TVOCs, during reference field test at indoor test location 6 (Leke)

The resulted average TVOC concentrations and the estimated relative difference between the indoor@box and the reference method (Radiello) from the reference field test performed at indoor test location 6 are shown Table 38Table 36.

Table 38 Resulted TVOC concentrations and the estimated relative difference obtained during the reference field test

	Radiello	indoor@box
Sampling period	7 days (13/03 – 20/03)	7 days (13/03 – 20/03)
TVOCs (average), µg/m³	119 µg/m³	145 ± 41 µg/m³
Relative difference between the TVOCs averages measured by the reference technique (Radiello) and indoor@box	22%	

4.1.7.4.5 Indoor test environment 7 (Koekelare)

The time series of the measurements from the indoor@box during the reference field test at indoor environment 7 (Koekelare) are shown in Figure 57.

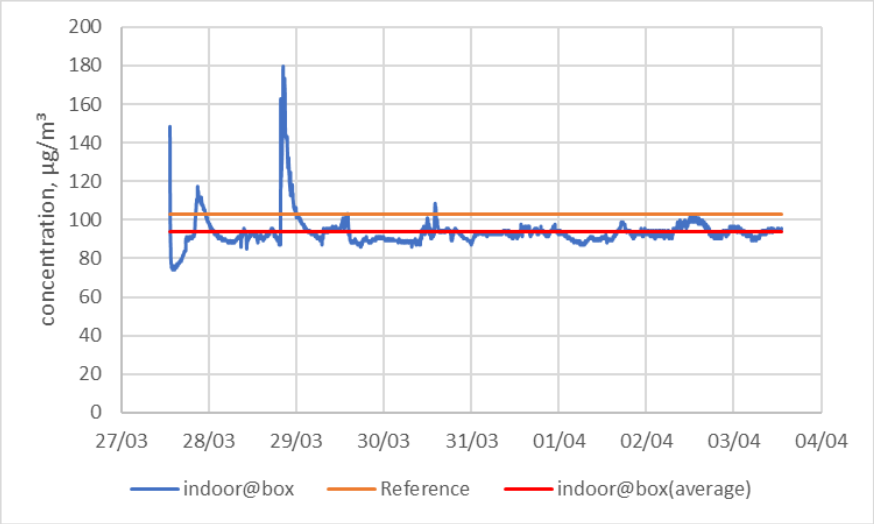

Figure 57 Time series of data obtained from indoor@box and reference measurement technique (Radiello) for TVOCs, during reference field test at indoor test location 7 (Koekelare)

The resulted average TVOC concentrations and the estimated relative difference between the indoor@box and the reference method (Radiello) from the reference field test performed at indoor test environment 7 are shown Table 39Table 36.

Table 39 Resulted TVOC concentrations and the estimated relative difference obtained during the reference field test

	Radiello	indoor@box
Sampling period	7 days (27/03 – 03/04)	7 days (27/03 – 03/04)
TVOCs (average), µg/m³	103 µg/m³	94 ± 8 µg/m³
Relative difference between the TVOCs averages measured by the reference technique (Radiello) and indoor@box	- 9%	

4.1.7.4.6 Indoor test environment 8 (Mariakerke)

The time series of the measurements from the indoor@box during the reference field test at indoor environment 8 (Mariakerke) are shown in Figure 58.

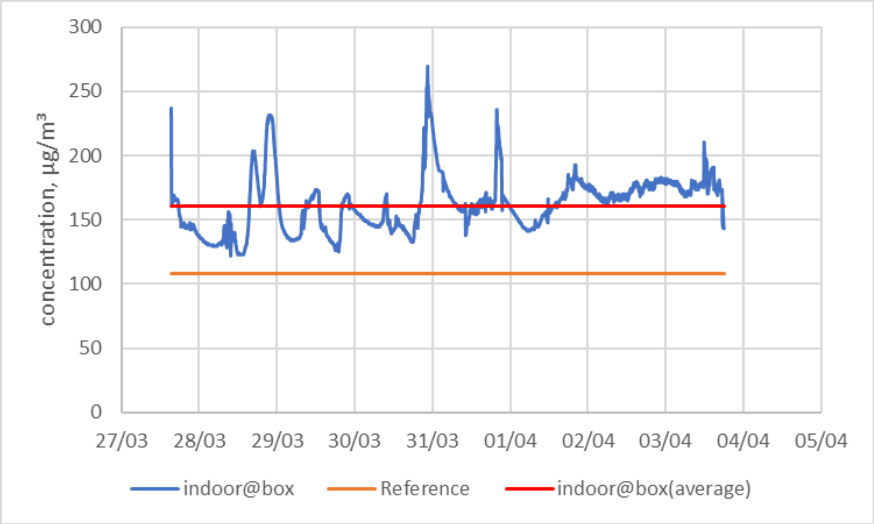

Figure 58 Time series of data obtained from indoor@box and reference measurement technique (Radiello) for TVOCs, during reference field test at indoor test location 8 (Mariakerke)

The resulted average TVOC concentrations and the estimated relative difference between the indoor@box and the reference method (Radiello) from the reference field test performed at indoor test location 8 (Mariakerke) are shown Table 40Table 36.

Table 40 Resulted TVOC concentrations and the estimated relative difference obtained during the reference field test

	Radiello	indoor@box
Sampling period	7 days (27/03 – 03/04)	7 days (27/03 – 03/04)
TVOCs (average), µg/m³	108 µg/m³	160 ± 23 µg/m³
Relative difference between the TVOCs averages measured by the reference technique (Radiello) and indoor@box	48%	

4.1.7.4.7 Indoor test environment 9 (Deftinge)

The time series of the measurements from the indoor@box during the reference field test are shown in Figure 59.

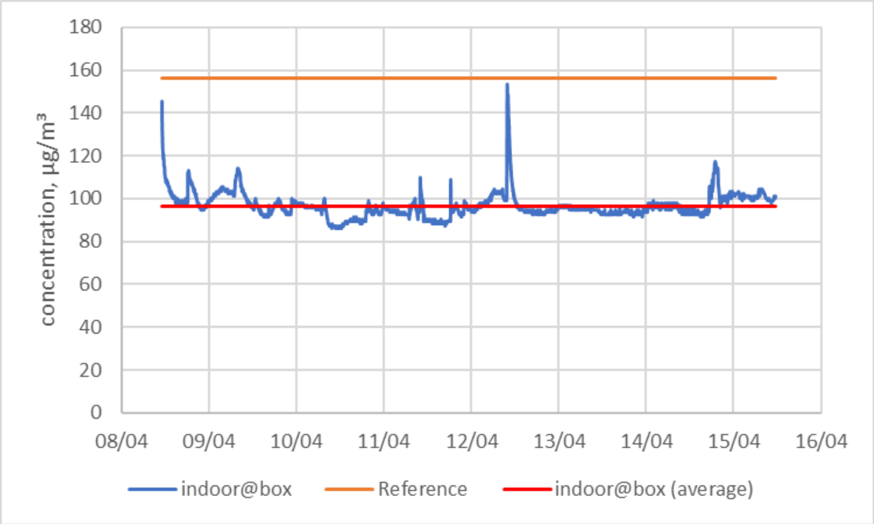

Figure 59 Time series of data obtained from indoor@box and reference measurement technique (Radiello) for TVOCs, during reference field test at indoor test location 9 (Deftinge)

The resulted average TVOC concentrations and the estimated relative difference between the indoor@box and the reference method (Radiello) from the reference field test performed at indoor test environment 9 are shown Table 41
Table 36.

Table 41 Resulted TVOC concentrations and the estimated relative difference obtained during the performed reference field test

	Radiello	indoor@box
Sampling period	7 days (08/04 – 15/04)	7 days (08/04 – 15/04)
TVOCs (average), µg/m³	156 µg/m³	97 ± 6 µg/m³
Relative difference between the TVOCs averages measured by the reference technique (Radiello) and indoor@box	- 38%	

4.1.7.4.8 Indoor test environment 10 (Schelle)

The time series of the measurements from the indoor@box during the reference field test are shown in Figure 60.

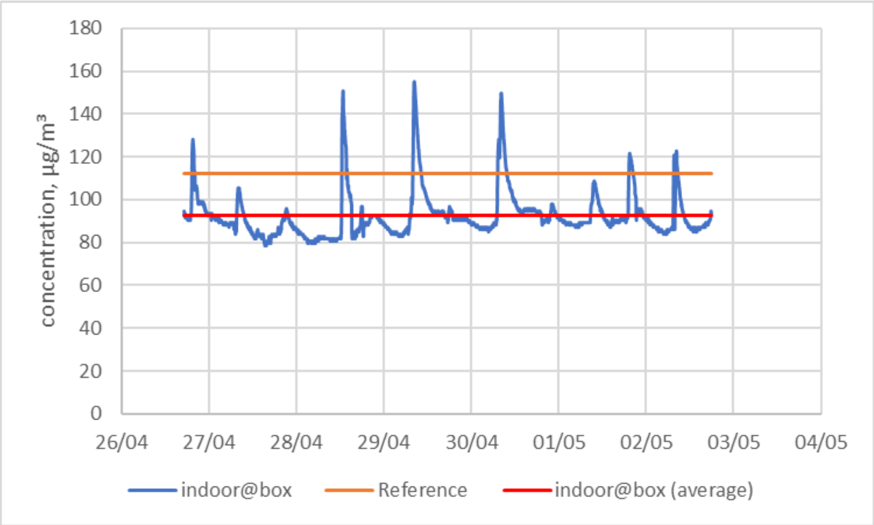

Figure 60 Time series of data obtained from indoor@box and reference measurement technique (Radiello) for TVOCs, during reference field test at indoor test environment 10 (Schelle)

The resulted average TVOC concentrations and the estimated relative difference between the indoor@box and the reference method (Radiello) from the reference field test performed at indoor test environment 10 are shown Table 42.
Table 36.

Table 42 Resulted TVOC concentrations and the estimated relative difference obtained during the performed reference field test at indoor test environment 10 (Schelle)

	Radiello	indoor@box
Sampling period	7 days (26/04 – 02/05)	7 days (26/04 – 02/05)
TVOCs (average), µg/m³	112 µg/m³	92 ± 11 µg/m³
Relative difference between the TVOCs averages measured by the reference technique (Radiello) and indoor@box	- 17%	

4.1.7.5 Carbon monoxide

The results from the reference field tests for carbon monoxide at different test environments are shown below. The values from the indoor@box devices presented in these plots have been corrected regarding the linear regression model obtained during the calibration process of the CO sensor under laboratory conditions.

4.1.7.5.1 Indoor test environment 6 (Leke)

The outcomes of the measurements from the indoor@box devices and reference monitor, during the reference field test at indoor test environment 6 (Leke) are shown in Figure 61, as time series and orthogonal regression plot.

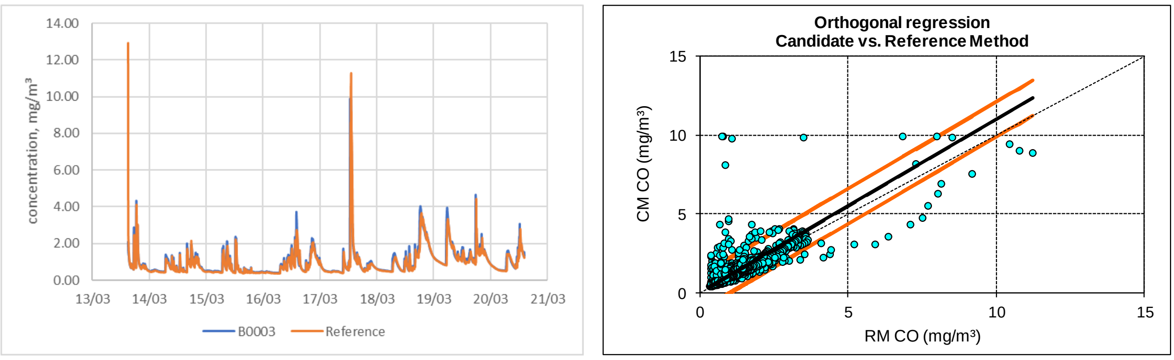

A B

Figure 61 Time series (A) and an orthogonal regression plot (B) of the measurements from the reference CO monitor (RM) and indoor@box (CM) during reference field test in indoor test environment 6 (Leke).

The resulted combined and expanded relative uncertainty of the compatibility of the measurements obtained from the indoor@box device with the reference CO monitor for defined limit value of 8 mg/m³ are shown in Table 43.

Table 43 Estimated uncertainties from the CO reference field test of indoor@box. The measurements of the indoor@box were corrected regarding the linear model estimated during lab calibration.

	Carbon monoxide
Combined uncertainty (u_{CR}), mg/m³	0.79
Combined relative uncertainty at limit value of 8 mg/m³ ($w_{CM,field}$), %	9.9
Expanded relative uncertainty at limit value of 8 mg/m³ ($W_{CM,field}$), %	19.8

4.1.7.5.2 Indoor test environment 8 (Mariakerke)

The outcomes of the measurements from the indoor@box devices and reference monitor, during the reference field test at indoor test environment 8 (Mariakerke) are shown in Figure 62, as time series and orthogonal regression plot.

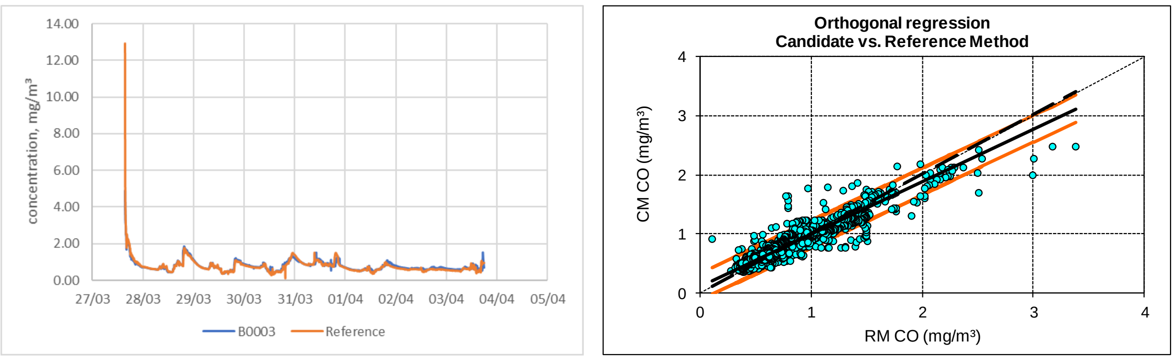

A B

Figure 62 Time series (A) and an orthogonal regression plot (B) of the measurements from the reference CO monitor (RM) and indoor@box (CM) during reference field test in indoor test environment 8 (Mariakerke).

The resulted combined and expanded relative uncertainty of the compatibility of the measurements obtained from the indoor@box device with the reference CO monitor for defined limit value of 8 mg/m³ are shown in Table 44.

Table 44 Estimated uncertainties from the CO reference field test of indoor@box . The measurements of the indoor@box were corrected regarding the linear model estimated during lab calibration.

	Carbon monoxide
Combined uncertainty (u_{CR}), mg/m³	0.77
Combined relative uncertainty at limit value of 8 mg/m³ ($w_{CM,field}$), %	9.6
Expanded relative uncertainty at limit value of 8 mg/m³ ($W_{CM,field}$), %	19.2

4.1.7.5.3 Indoor test environment 9 (Deftinge)

The outcomes of the measurements from the indoor@box devices and reference monitor, during the reference field test at indoor test environment 9 (Deftinge) are shown in Figure 63, as time series and orthogonal regression plot.

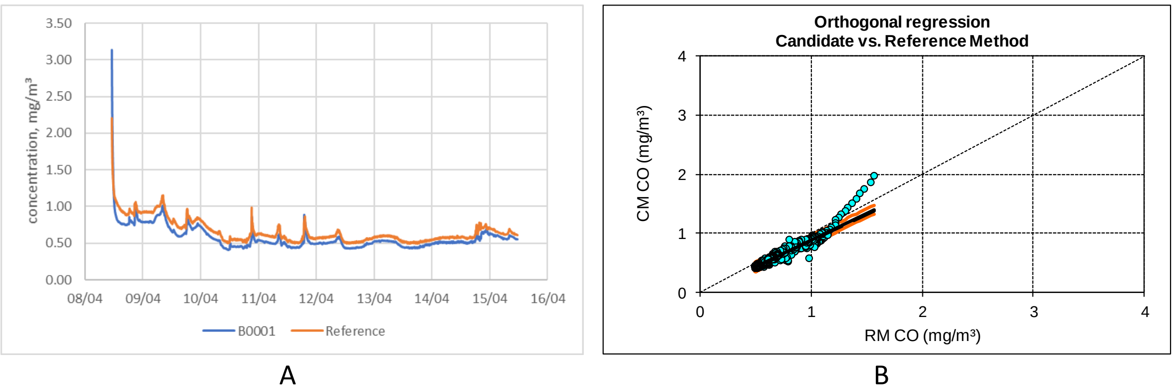

Figure 63 Time series (A) and an orthogonal regression plot (B) of the measurements from the reference CO monitor (RM) and indoor@box (CM) during reference field test in indoor test environment 9 (Deftinge).

The resulted combined and expanded relative uncertainty of the compatibility of the measurements obtained from the indoor@box device with the reference CO monitor for defined limit value of 8 mg/m³ are shown in Table 45.

Table 45 Estimated uncertainties from the CO reference field test of indoor@box . The measurements of the indoor@box were corrected regarding the linear model estimated during lab calibration.

	Carbon monoxide
Combined uncertainty (u_{CR}), mg/m³	0.75
Combined relative uncertainty at limit value of 8 mg/m³ ($w_{CM,field}$), %	9.4
Expanded relative uncertainty at limit value of 8 mg/m³ ($W_{CM,field}$), %	18.8

The results presented above, showed that the obtained combined and extended relative uncertainties of the tested indoor@box devices estimated at limit value of 8 mg/m³ were within the maximal allowed uncertainty of 30% for indicative measurements of inorganic gasses (e.g. nitrogen dioxide, sulphur dioxide, carbon monoxide) in ambient air quality assessments (Directive 2008/50/EC (Parliament 2008)).

4.1.7.6 Light intensity

The time series and the orthogonal regression plot of the data obtained from the indoor@box and reference monitor (Testo 545), during the reference field tests for light intensity are shown inFigure 64. The values from the indoor@box presented in these plots have been corrected regarding the linear regression model obtained during the calibration process of the light intensity sensors at laboratory conditions.

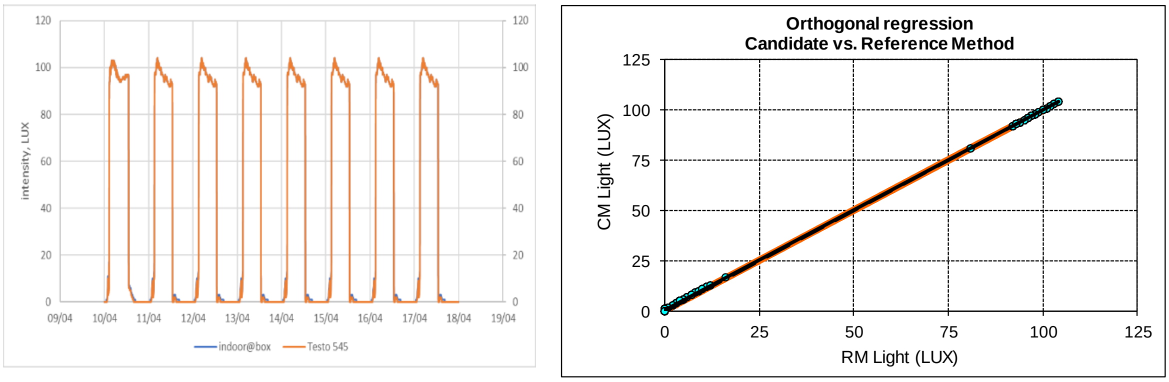

Figure 64 Time series and an orthogonal regression plots of the measurements from the reference light intensity monitor (RM) and indoor@box (CM) during reference field test in indoor test environment 1 (Mol).

The resulted combined and expanded relative uncertainty of the compatibility of the measurements obtained from the indoor@box device with the reference light intensity monitor (Testo 545) for defined limit value of 1000 lux are shown in Table 46.

Table 46 Resulted uncertainty from the light intensity reference field test of indoor@box . The measurements of the indoor@box were corrected regarding the linear model estimated during lab calibration.

	Light intensity
Combined uncertainty (u_{CR})	0.83 lux
Combined relative uncertainty at limit value of 1000 lux ($w_{CM,field}$)	0.08 %
Expanded relative uncertainty at limit value of 1000 lux ($W_{CM,field}$)	0.6 %

The expanded relative uncertainty of the parameter is very low since the sensor used in the indoor@box uses similar technology to measure light intensity as the reference device (Testo 545).

5 CONCLUSION

The overall outcomes from the initial field test i.e. evaluation between indoor@box uncertainties of the available indoor@box devices showed relatively comparable outcomes. The sensors used for measuring CO_2, T, RH and TVOC comply with the pre-defined objective criteria of 20% for relative between instrument uncertainty defined for this assessment.

In term of the comparison between the measurement of the selected parameters from the indoor@box devices with the reference measurement techniques performed at real indoor environments, the indoor@box devices showed very comparable results. Combined relative uncertainties of below 30% at the defined limit values were observed for most of the tested parameters (e.g. T, RH, CO_2, light intensity, TVOC). Although, the combined relative uncertainty for PM was estimated to be larger than 30%, it was still below the limit value of 50% defined by Directive 200/50/EC (Parliament 2008) as a data quality objective for indicative measurements for ambient air quality assessment.

The results obtained during these field studies showed that the tested indoor@box devices can be successfully used for providing supplemental (indicative) measurements to the existing reference techniques for CO_2, T, RH, TVOC and light intensity and to some extend PM_1, $PM_{2.5}$ and PM_{10} (regarding the corresponding relative uncertainty) assessment in indoor environments.

In addition, the performed experiments of applying the field calibration model to the data obtained from the indoor@box showed that the uncertainty of the results could be reduced significantly. This method of field validation, however, is valid and limited only to the location where the field validation of the used indoor@box device was performed.
It is important to be mentioned here, that all the outcomes and conclusions resulted from the described in this report experiments are limited to the tested indoor@box devices and the corresponding indoor test environments. To be able to make more definitive conclusion regarding the applicability of the developed during this project concept of monitoring device for indoor environmental quality assessments, the described field experiments in this report shall to be extended to additional number of devices and indoor environments.

REFERENTIES

Benabed, A. and K. Limam (2017). "Resuspension of Indoor Particles Due to Human Foot Motion." *Energy Procedia* **139**: 242-247.

Commission, E. (2010). Guide to the demonstration of equivalence of ambient air monitoring methods. Report by an EC Working Group on Guidance for the Demonstration of Equivalence.

Parliament, E. (2008). DIRECTIVE 2008/50/EC OF THE EUROPEAN PARLIAMENT AND OF THE COUNCIL of 21 May 2008 on ambient air quality and cleaner air for Europe. Official Journal of the European Union. Brussels. **L152/1**.

Spinelle, L., M. Aleixandre and M. Gerboles (2013). "Protocol of evaluation and calibration of low-cost gas sensors for the monitoring of air pollution."

Spinelle, L., M. Gerboles and M. Aleixandre (2015a). "Performance Evaluation of Amperometric Sensors for the Monitoring of O3 and NO2 in Ambient Air at ppb Level." *Procedia Engineering* **120**: 480-483.

Spinelle, L., M. Gerboles, M. G. Villani, M. Aleixandre and F. Bonavitacola (2015b). "Field calibration of a cluster of low-cost available sensors for air quality monitoring. Part A: Ozone and nitrogen dioxide." *Sensors and Actuators B: Chemical* **215**: 249-257.

E+E Electronik (2015) Datasheet: EE893 Digital CO_2 Sensor Module for OEM Applications. http://www.epluse.com/fileadmin/data/product/ee893/Datasheet_EE893.pdf

Texas Instruments (2017) Datasheet: ADS111x Ultra-Small, Low-Power, I2C-Compatible, 860-SPS, 16-Bit ADCs With Internal Reference, Oscillator, and Programmable Comparator (Rev. C). http://www.ti.com/product/ADS1115/datasheet

Shinyei (2013) Product Specifications: PPD60PV-T2 Particulate Matter Sensor.

Microchip (2016) ATmega328 Microchip picoPower 8-bit AVR RISC-based microcontroller. http://www.microchip.com/wwwproducts/en/ATmega328P

Sensirion (2011) Datasheet SHT7x (SHT71, SHT75) Humidity and Temperature Sensor IC. https://www.sensirion.com/fileadmin/user_upload/customers/sensirion/Dokumente/Humidity_Sensors/Sensirion_Humidity_Sensors_SHT7x_Datasheet_V5.pdf

Spinelle L. et al. (2015a) Field calibration of a cluster of low-cost available sensors for airquality monitoring. Part A: Ozone and nitrogen dioxide. Sensors and Actuators, B215, 249-257

Spinelle L. et al. (2015b) performance evaluation of amperometric sensors for the monitoring of O_3 and NO_2 in ambient air in ppb levels. Procedia Engineering, 120, 480-483

Alphasense (2016a) Technical specifications: PID Photo Ionisation Detector. http://www.alphasense.com/index.php/products/pid/

AMS (2016) Technical specification: TSL2560, TSL2561 Light-to-Digital Converters. http://ams.com/eng/content/download/250094/975485/file/TSL2560-61_DS000110_2-00.pdf

Alphasense (2015) Technical specifications: CO-B4 Carbon monoxide sensor 4-electrode. http://www.alphasense.com/WEB1213/wp-content/uploads/2015/04/COB41.pdf

OpenEnergyMonitor (2016) Technical wiki EmonTx V3.4. https://wiki.openenergymonitor.org/index.php/EmonTx_V3.4

Alphasense (2016d) Technical specifications: NO2-B43F Nitrogen Dioxide Sensor 4-Electrode http://www.alphasense.com/WEB1213/wp-content/uploads/2016/07/NO2-B43F.pdf

Sauter (2015) Instruction Manual Digital Sound Level Meter. https://dok.kern-sohn.com/manuals/files/English/SU-BA-e-1512.pdf

ETSI EN 300 440 V2.1.1 (2017) Short Range Devices (SRD); Radio equipment to be used in the 1 GHz to 40 GHz frequency range; Harmonised Standard covering the essential requirements of article 3.2 of Directive 2014/53/EU http://www.etsi.org/deliver/etsi_en/300400_300499/300440/02.01.01_60/en_300440v020101p.pdf

Kang, J. and K.-I. Hwang (2016). "A Comprehensive Real-Time Indoor Air-Quality Level Indicator." Sustainability 8(9): 881.

Sef van den Elshout, Hans Bartelds, Hermann Heich, Karine Léger (2012) CAQI Air quality index, (https://www.airqualitynow.eu/index.php)

Syazwan, A. I., et al. (2012). "Development of an indoor air quality checklist for risk assessment of indoor air pollutants by semiquantitative score in nonindustrial workplaces." Risk Management and Healthcare Policy 5: 17-23.

ANNEX A ELECTRONIC SCHEME OF INDOOR@BOX'S SENSOR CONTROLLER UNIT

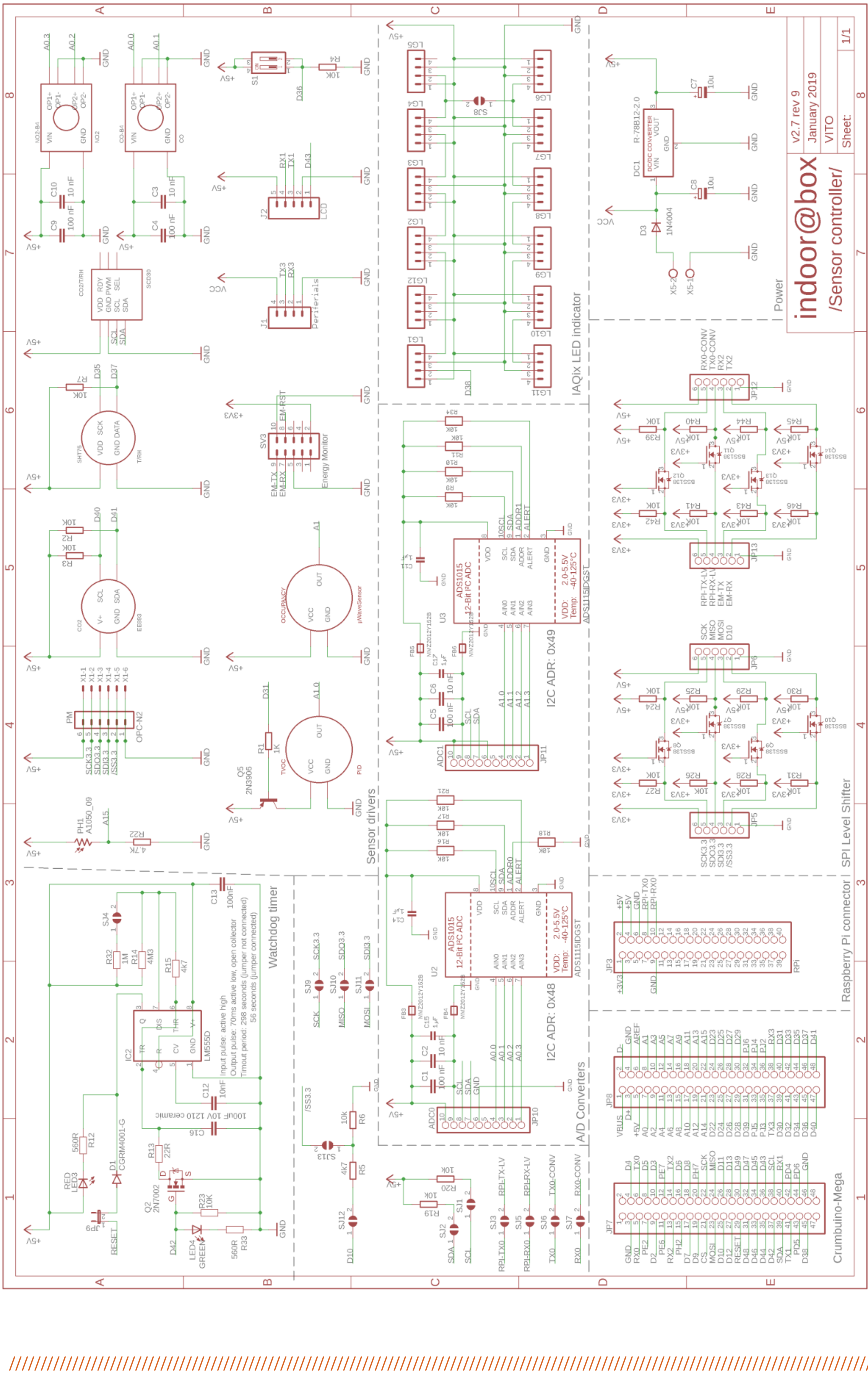

SENSOR CONTROLLING UNIT'S COMMUNICATION PROTOCOL

1. *Sensor controlling unit's communication protocol overview*

This document describes the communication protocol between Indoor@box 's sensor controller unit and processing unit and associated firmware release.

Document version: 1.0 – 06.2017

2. *Physical layer*

The communication with the sensor controller unit is made through a serial line running at 9600bps, 8 bit, no parity. Line level is 5V (TTL).

3. *Communication syntax*

The sensor controller unit could accept a set of commands. Each command set is defined by a frame. A frame is limited by braces containing a letter and two or more digits. Commands are identified by a letter and are case sensitive. The sensor controller unit acknowledges each command by repeating the command itself and appending result values, if any. Each error or not valid command is acknowledged by the general string { * }

4. *Start and stop commands*

<u>Start sampling</u>

Purpose:	Start the sampling process
Command:	S
Parameters:	None
Results:	An acknowledgement of the command as soon as the sampling process started
Example:	
Tx:	{S}
Rx:	{S}

ANNEX C IAQIX CALCULATION ALGORITHM

The IAQix developed for the indoor@box sensors device define four main IAQix levels focused on the health effects of the selected pollutant. The four main IAQix levels are assigned as: “Good”; “Moderate”; “Unhealthy”; and “Very Unhealthy” (Table 47).

Table 47 IAQix levels and corresponding concentration breakpoints defined for indoor@box

Level/Category description	A Good		B Moderate		C Unhealthy		D Very Unhealthy	
Values I_{LO}	0		50		100		250	
Values I_{HI}	50		100		250		500	
Parameter	BP_{LO}	BP_{HI}	BP_{LO}	BP_{HI}	BP_{LO}	BP_{HI}	BP_{LO}	BP_{HI}
VOC (µg/m³)	0	299	300	999	1000	4999	5000	15000
CO (ppm)	0	2.9	3	4.9	5	6.9	7	88
PM (µg/m³)	0	9.9	10	24.9	25	99	100	300
NO_2 (µg/m³)	0	19.9	20	39.9	40	199	200	400

Based on the measured concentration from the sensors of the indoor@box , the individual (IAQ) index of each of the selected parameters is calculated following eq. (1). This calculation simply converts a concentration value from a sensor into generalized index value with respect to its breakpoint. Since the characteristics and value of each pollutant are different, the breakpoint of each level is individually determined with respect to the guideline and intervention concentration levels listed in the Vlaamse Binnenmilieubesluit (2018) (Table 48). All the values of the breakpoints of each parameter are shown in Table 47.

$$I_{(n)} = \frac{I_{HI} - I_{LO}}{BP_{HI} - BP_{LO}}(C - BP_{LO}) + I_{LO} \quad (1)$$

$I_{(n)}$	The (Air-quality) index of pollutant *n*
C	The pollutant concentration
BP_{LO}	The concentration breakpoint that is ≤ C
BP_{HI}	The concentration breakpoint that is ≥ C
I_{LO}	The index breakpoint corresponding to BP_{LO}
I_{HI}	The index breakpoint corresponding to BP_{HI}

Based on the individual (IAQ) level for each parameter, the IAQix is determined. In general, the worst individual index of all pollutants becomes the IAQix. In addition, if there two or more pollutant that show an “Unhealthy” level, an additional weight is added to the pollutant with the worst individual index. For example, if there two “Unhealthy” levels, 25 is added to the calculated IAQix. If there are three or four “Unhealthy” levels, 50 and respectively 75 is added to the calculated IAQix.

Table 48 Guideline and intervention concentration levels fort he selected IAQ parameters listed in the Vlaamse Binnenmilieubesluit (2018).

Parameter	Richtwaarde	Interventiewaarde
VOC (µg/m³)	300	1000
CO (ppm)	-	6.98
PM (µg/m³)	10	-
NO_2 (µg/m³)	20	40

Example 1:

Parameter	Measured concentrations	$I_{(n)}$	Weight	IAQix
VOC (µg/m³)	500	**64**	**0** (Zero "Unhealthy" levels)	**84** (Moderate)
CO (ppm)	2.0	**34**		
PM (µg/m³)	20	**84**		
NO_2 (µg/m³)	20	**50**		

Example 2:

Parameter	Measured concentrations	$I_{(n)}$	Weight	IAQix
VOC (µg/m³)	500	**200**	**25** (Two "Unhealthy" levels)	**204** (Unhealthy)
CO (ppm)	2.0	**6.0**		
PM (µg/m³)	20	**20**		
NO_2 (µg/m³)	20	**30**		

Example 3:

Parameter	Measured concentrations	$I_{(n)}$	Weight	IAQix
VOC (µg/m³)	500	**200**	**50** (Two "Unhealthy" levels)	**300** (Very Unhealthy)
CO (ppm)	2.0	**6.0**		
PM (µg/m³)	20	**20**		
NO_2 (µg/m³)	20	**200**		